Electron beam etching

Drenth, S.

Award date:
1985

Technische Hogeschool Eindhoven

Afdeling der Technische Natuurkunde

Vakgroep Vaste Stof Fysica

Onderwerpgroep Fysica van Oppervlakken en Grenslagen

Electron Beam Etching

S. Drenth

Afstudeer verslag van S. Drenth.

Afstudeerhoogleraar : prof.dr. H.H. Brongersma.

Met dank aan alle mensen van de F.O.G. groep die mij vaak met raad en daad hebben bijgestaan en met wie ik vele interessante en gezellige discussies heb mogen voeren. Speciale dank echter voor Louis Saes voor de uitstekende hulp aan het einde van deze afstudeerperiode.

S. Drenth

Eindhoven, februari 1985.

Summary.

In recent years there exists a growing interest in the miniaturization of integrated circuits. This is clear from the efforts undertaken in the investigation of new etching techniques. In this way the plasma etching technique already is a successor of the wet etching technique. The obtainable accuracy in the wet etching technique is about 3 μm while in the plasma etching technique 0.5 μm can be reached. But there still is a large demand for higher accuracies.

The limitting factor for the accuracy in the plasma etching technique is formed by the necessity of a fotomask because of the global character of the process. If higher accuracies are needed the fotomask must be abandoned. The etching process must thus be a local one.

It was thought that such a local etching process could be obtained with an electron beam. As an additional component an etchgas is needed to realise an etching process.

In this work a model for such a process is worked out. It shows that secondary electrons play an important role. Their properties determine whether the surface charges positive or negative under the influence of an electron bombardment. This, on its turn, decides which ions can etch the surface.

From the experiments carried out with SiO_2 it is clear that the etching process depends strongly on the accelerating voltage of the electron beam. From these results it could be concluded that only F^+ ions are able to etch the SiO_2 surface. Beside that it shows that oxygen might have a negative influence on the velocity of the etching process.

From calculations in a simplified model it may be concluded that the accuracy of the etching process is only limited by the dimensions of the electron beam.

The maximum obtained efficiency is low, 1 %. This means that 100 incident electrons are needed to remove 1 SiO_2 molecule from the surface. This causes long etching times if large areas must be etched.

However, since the long etching time is inherent to the local character of the etching process and its high accuracy this process could be of use as an addition to e.g. plasma etching.

Many questions are still unanswered and thus continued research is necessary.

Contents.

Chapter 0: Introduction

0.1 : General

Nowadays integrated circuits are widely used in all kinds of apparatus ranging from a lathe to a computer.
These chips take dull, laborious and difficult work away from the users, so this work can be done faster and more accurate.

These I.C.s, however, are never quick enough, accurate enough nor small enough. Think for instance of computers. There is a continuous demand for faster computers with larger data storage capacities and, of course, smaller dimensions.
These demands can partly be fulfilled by using higher clock frequencies and placing more I.C.'s on the circuit board. But there is a limit to these methods and if this limit is reached the only thing that can be done to fulfill these demands is using a higher degree of integration.

Some years ago (± 1980) the only technique used for the I.C.-production was the wet etching technique. With this technique one can reach an accuracy in the range of 2 to 4 microns. (WAR65) It is very difficult to reach higher resolutions with this process because of some fundamental properties of it. (KEL78) (See also paragraph 0.2)

At that time, however, there was no need for a higher resolution. A higher resolution would mean a higher degree of integration and that would mean more components on the same area. This in its turn would mean an increased heat-production if the same materials and techniques were used.

Nowadays the heatproduction can be reduced by using new techniques and the heat can be removed more efficiently (e.g. heatpipes). So it now becomes useful to develop etch techniques with higher resolutions (e.g. plasma etching).

0.2 : Wet etching and plasma etching

The principles of the wet etching process are shown in figure 0.1 .

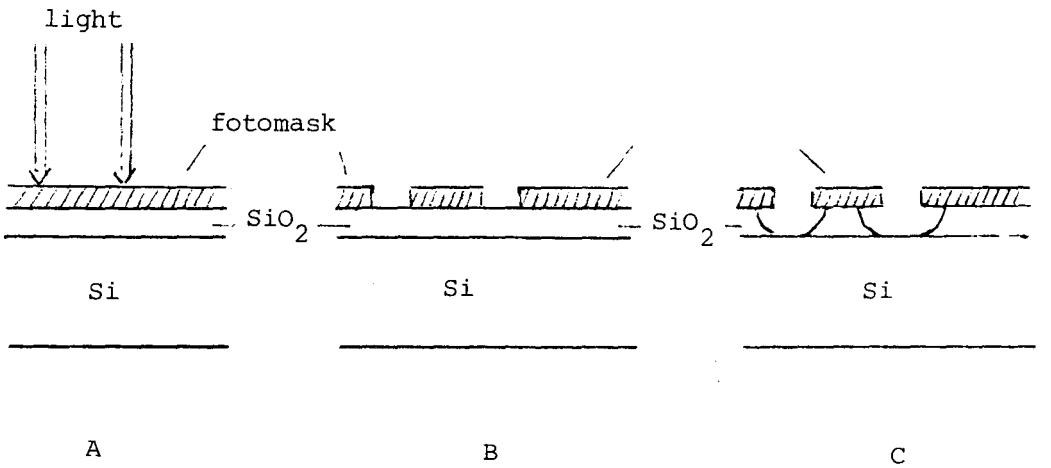

fig. 0.1. : Principles of the wet etching process.

In fig. 0.1.a the fotosensitive but etchant resistive top layer is illuminated on the place which must be etched. After the development of that fotographic layer the etch mask is left on the SiO_2 surface as is shown in fig. 0.1.b. Now the SiO_2 is removed through the holes of the mask by an etching liquid down to the Si layer (fig. 0.1.c.). If necessary the Si substrate can then be etched by a selective etching procedure. After the removal of the etch mask the wafer (= the slice) is prepared for the next step, e.g. local diffusion (WAR65).

This process has two disadvantages, namely :

1. the need of an etch mask,
2. the pressence of underetching (see fig. 0.2).

The phenomenon of underetching is explained in figure 0.2.

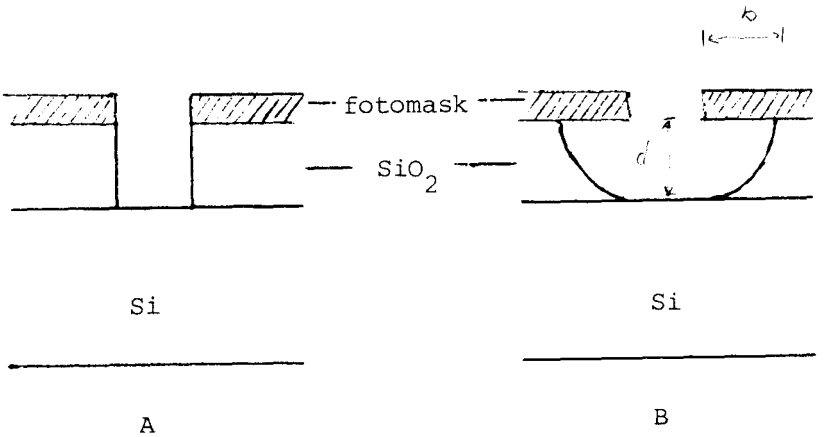

fig. 0.2. : A : Ideal etch case.
B : Underetching due to omnidirectional etching.

The ideal situation is shown in fig. 0.2.a. : sharp edges normal to the Si substrate. In fig. 0.2.b. is shown what happens in reality. This effect is called underetching and originates from the essentially omnidirectional nature of the wet etching process ($p \sim d$).

This phenomenon (underetching) and the occurance of small gasbubbles on the SiO_2 during the wet etching process (KEL78) are the fundamental reasons why high resolutions cannot be obtained in the wet etching process.

Concerning the high resolution, an improvement of the wet etching is the plasma etch technique. The first phase of the process is the same as for wet etching, a fotomask has to be applied to the SiO_2 surface.
The essential difference lies in the method of etching.

Plasma ethcing takes place in vacuum. A glow discharge is made in an etchgas just above the surface. Often CF_4, SiF_4 and SF_6 are used as etch gas. In that glow discharge

(plasma) F ions are produced. They impinge on the SiO_2 surface. On those places where the SiO_2 is not covered with a mask the F^+ ions are believed to react with the Si atoms to SiF_2 (FLA81) and SiF_4 (COB79). These products are both gaseous and thus escape from the surface.

Because of the charging of the surface by electrons from the plasma, the F^+ ions obtain a velocity normal and towards the surface. Because of this, and some additional techniques (COB79), only very little underetching occurs. So higher resolutions, up to 0.5 micron, can be obtained.

But there are also disadvantages to this technique:

1. an etchmask is still needed
2. the Si bulk can be damaged by the radiation of the glow discharge,
3. the Si bulk can be damaged by the impact of ions.

To avoid these disadvantages a local and directional etching technique is needed. This means that the etching spot should be tunable so no mask is needed anymore and high resolutions can be obtained.

Research carried out by prof. dr. H.H. Brongersma et.al. showed the possibility of local and directed etching with an electron beam. With an electron beam very fine spots can be made. So, viewed at in the light of the things descibed above, it seemed worth while to continue this research in order to acquire more knowledge about this electron beam etching process. That is what I have tried to do during this research project.

0.3. : The contents of this essay.

In chapter one first the principle idea behind the electron beam etch technique is described. Then the properties of secondary electrons, which play a fundamental role in the electron beam etching process, are discussed. With this knowledge a model is presented. Finally some specific properties of the fluoroacetic acid/silicondioxide system are treated because the model was tested with trifluoroacetic acid and silicondioxide.

In chapter two the experimental arrangements are described. A description of the most important parts is given.

In chapter three the results are displayed and discussed.

In chapter four a discussion of the results is given and the conclusions are drawn.

In appendix I some properties of trifluoroacetic acid and silicondioxide are listed.

In appendix II the colour chart of SiO_2 is listed.

Chapter 1 : Theory.

1.0. : Introduction.

In paragraph 1.1 the basic idea behind the electron beam etching process is presented.

Because the secondary electrons play a decisive role in this process, the properties of secondary electrons in general are dealt with in paragraph 1.2.
In the same paragraph the properties of metals, semiconductors and insulators concerning the production of secondary electrons are treated.

Then, in paragraph 1.3, the final model of the electron beam etch process can be presented, including some interesting remarks.

Since we are particularly interested in the etching of silicondioxide, paragraph 1.4 deals with some special subjects concerning this specific etching process. Section 1.4.1 of that paragraph deals with the choice of the etchgas and this chapter ends at section 1.4.2 where the adsorption properties of the chosen gasmolecules on silicondioxide are discussed.

1.1 : The basic principles of the local and directional electron beam etching process.

Etching without a mask requires a mechanism for local and directional etching. A pattern must be "written" in the surface. For instance with a well defined electron beam (e-beam).
But an e-beam alone does not etch the surface. It can only heat it, charge it or produce secondary electrons (see 1.2). Something additional is needed. Something that is adsorbed on the surface and is activated, to etch the surface, by the e-beam. After the etching process the reactionproducts must leave the surface and the adsorbate must be renewed. Because of the e-beam, the process takes place in vacuum, so the additional compound is a gas.

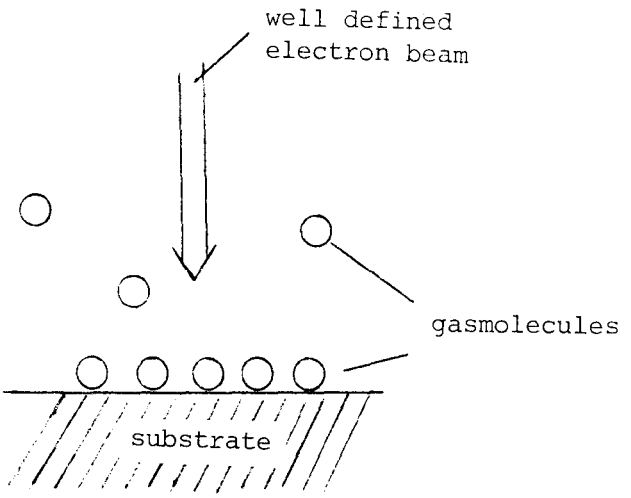

fig. 1.1. : Components necessary for the e-beam etching process

The gasmolecules themselves may not etch the surface unless they are activated by electrons.

To obtain high resolutions, as needed in VLSI production, the e-beam must be very well defined (spot on the surface of about 0.1 micron).
Focussing of the e-beam to such spot dimensions can, because of spacecharge effects, only be obtained with high energetic electrons (keV range).

However, this immediately leads to another problem.
Cross-sections for electron-molecule interactions are very small for those high energetic electrons (order of 10^{-20} cm^2).

Fortunately the energetic incident electrons (so called primary electrons) produce, at impact on the surface, secondary electrons (see : 1.2).*
These S.E. have an energy distribution with a maximum generally below 5 eV. (see fig. 1.2).

* Note: In the following we refer to primary electrons as P.E. and to secondary electrons as to S.E.

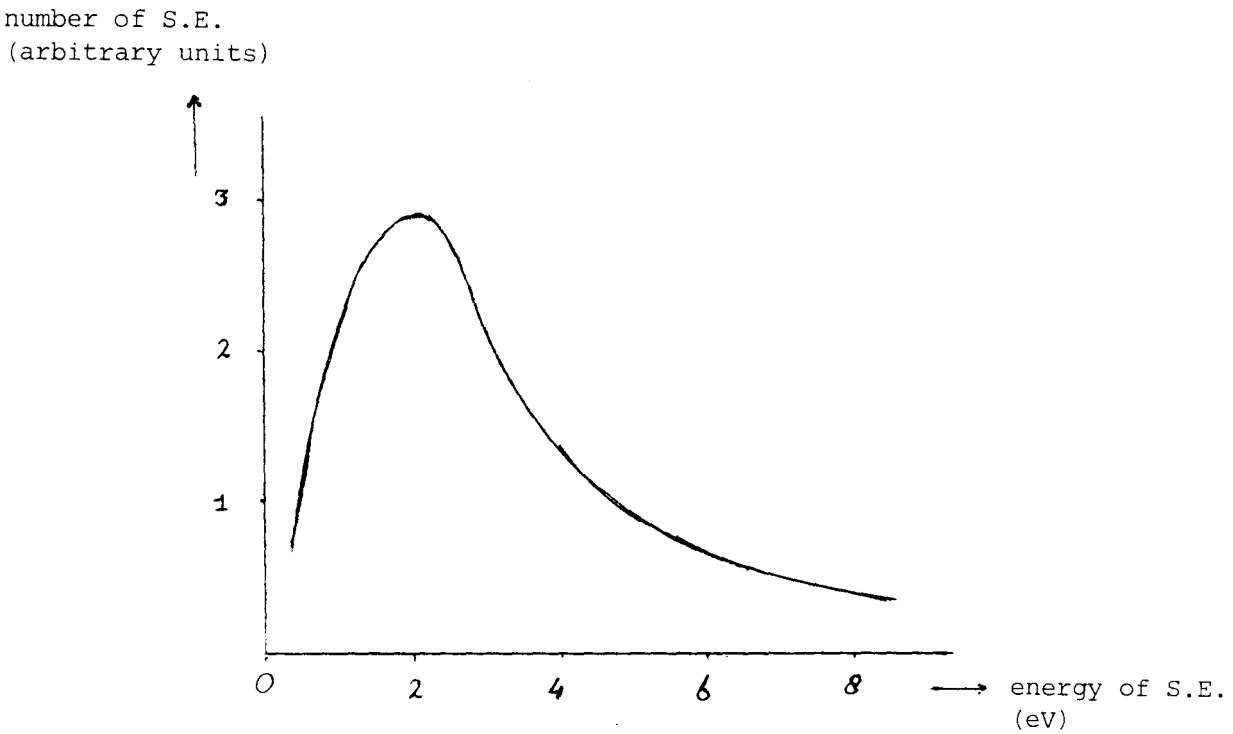

fig. 1.2. : General shape of a S.E. energy distribution function.

The overall basic thought behind the e-beam etch process is shown in fig. 1.3.a-e.

The specially selected gasmolecules can simply be looked at as consisting of two different parts, A and B.
The gasmolecules are adsorbed on the surface due to the special properties of part A (fig. 1.3.a). The gasmolecules themselves do not etch the surface, but they contain a reactive part, part B, that is able to react with the surface atoms.
Part B is splitt from the molecule on interaction of the molecule with a S.E. produced by incident P.E. (fig. 1.3.b,c). Then part A leaves the surface and part B is directed towards the surface. At the surface, part B forms a gaseous reaction product with a lifetime long enough to escape from the surface (fig. 1.3.d,e).After the adsorption of a fresh etchgas molecule the process can start again.

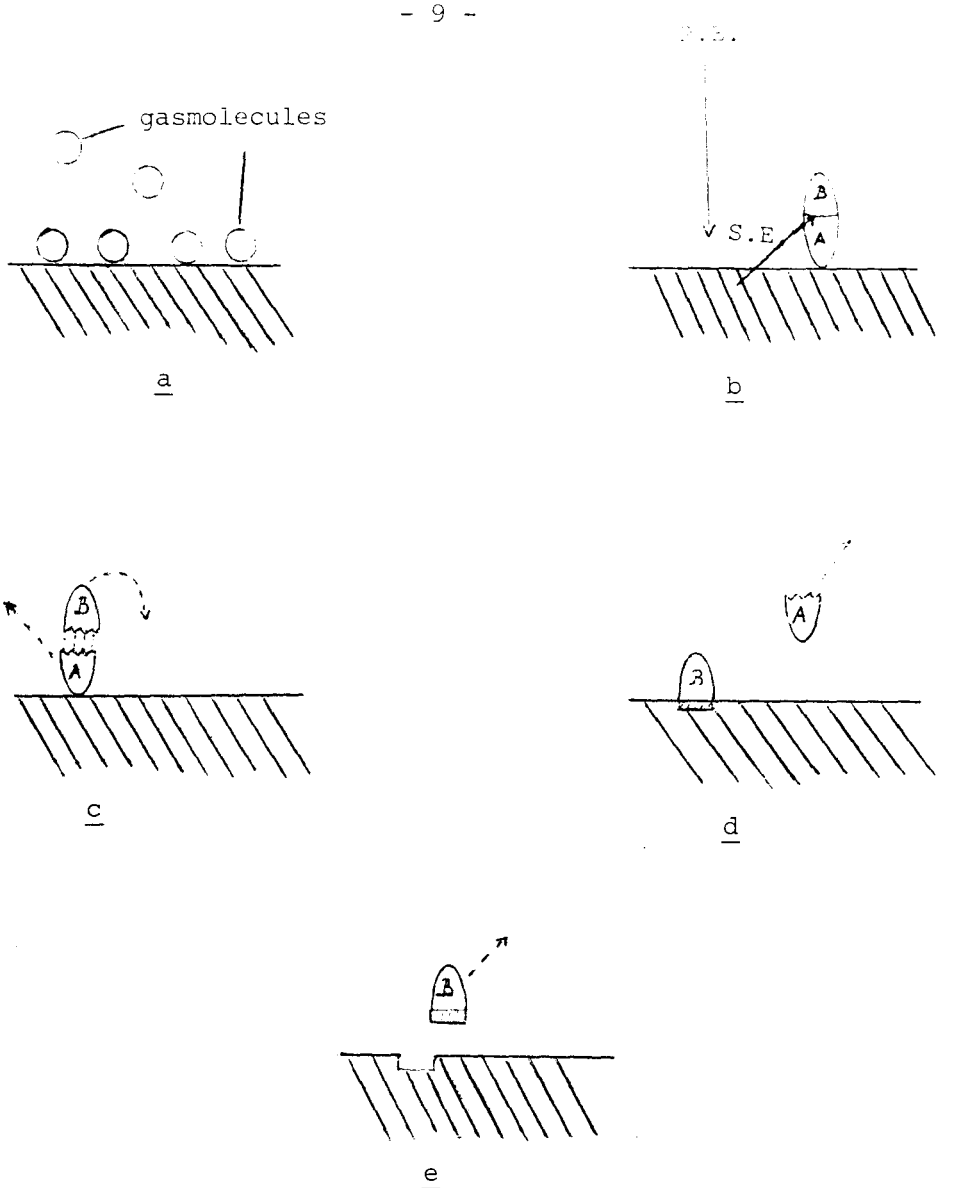

fig. 1.3. : The basic idea of the e-beam etching process.

a : gasmolecules adsorb on the surface,

b : the incident P.E. produce S.E.,

c : on interaction with S.E. the molecule splits in a reactive part B and a non-reactive part A that leaves the surface,

d : the reactive part B reacts with the surface,

e : the reaction product leaves the surface.

1.2. : Secondary Electrons.

1.2.0. : Introduction.

This paragraph will describe various properties of secondary electrons. This paragraph is divided into different sections :

Section 1.2.1. : this section deals with the general properties of secondary electrons.

Section 1.2.2. : in this section the charging of a target is discussed in relation to the properties of S.E.

Section 1.2.3. : this sections deals with the total yield of secondary electrons of metals, semiconductors and insulators.

Section 1.2.4. : in this section the influence of the angle of incidence of the P.E. on the total yield and angular distribution of the emitted S.E. is discussed.

Section 1.2.5. : in this section finally some special properties of insulators, concerning S.E. are discussed.

1.2.1. : General Properties.

Every material that is exposed to a bombardement of electrons will emit secondary electrons (S.E.).

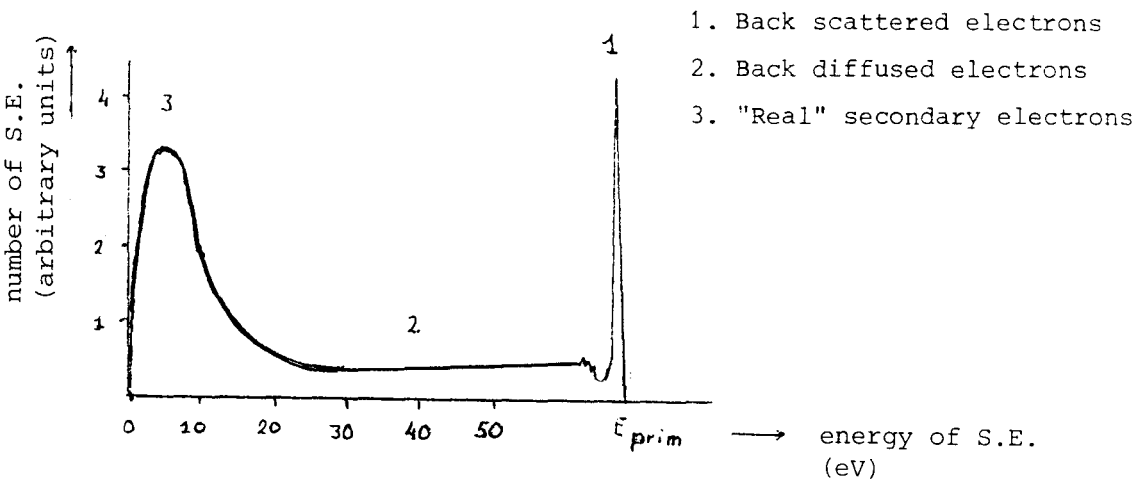

fig. 1.4. : Energy spectrum of, from the surface, emitted electrons when the surface is bombarded with primary electrons (P.E.) of energy E_{prim}. (GIB66)

In fig 1.4 a typical energy distibution curve of electrons emitted from a bombarded target is shown.
A number of features are immediately clear :

1. There is a very large maximum at the energy of the incident electrons. These may be distinguished as P.E. which have suffered elastic collisions with the lattice and have merely been reflected.
2. There are some subsidiary discrete maxima a few eV below the energy of the primary electrons. These are followed by an extended continuüm down to low energies.

These peaks are due to plasmon interactions.

The continuüm is due to electrons which have suffered inelastic collisions and are rediffused.

3. Further there is a maximum occuring at a few eV and falling to a low value at a few tens of eV.
   These electrons are termed "true" S.E.
   They are thought of as electrons which originally occupied bound states within the material. (KOL56)

The shape of the curve of fig. 1.6. is only valid if the energy of the P.E. is larger than 50 eV (KOL56).

An interesting and thus extensively investigated property of materials is the variation of the total yield Y of S.E. with the energy of the incident P.E.
The total yield Y is defined as the number of emitted S.E. divided by the number of incident P.E.

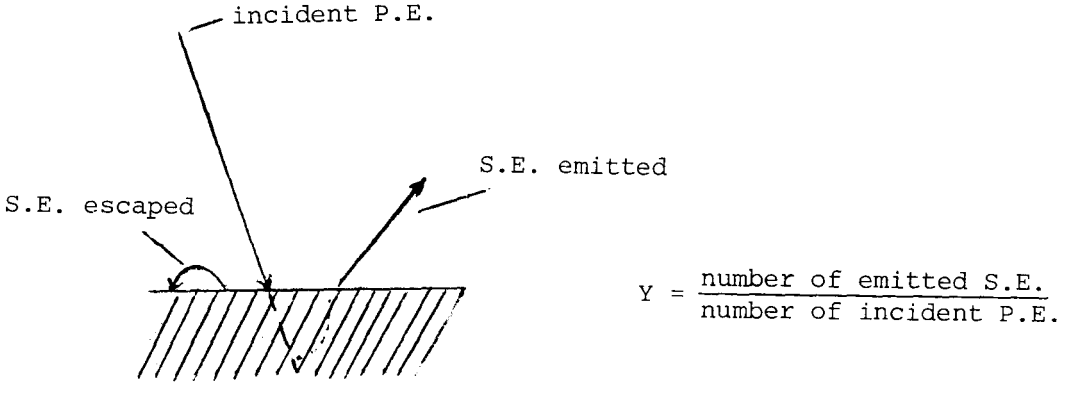

fig. 1.5. : Definition of the total yield Y.

The value of Y determines whether a surface, if it is kept floating, will charge positively or negatively under electron bombardement (see section 1.2.2.).

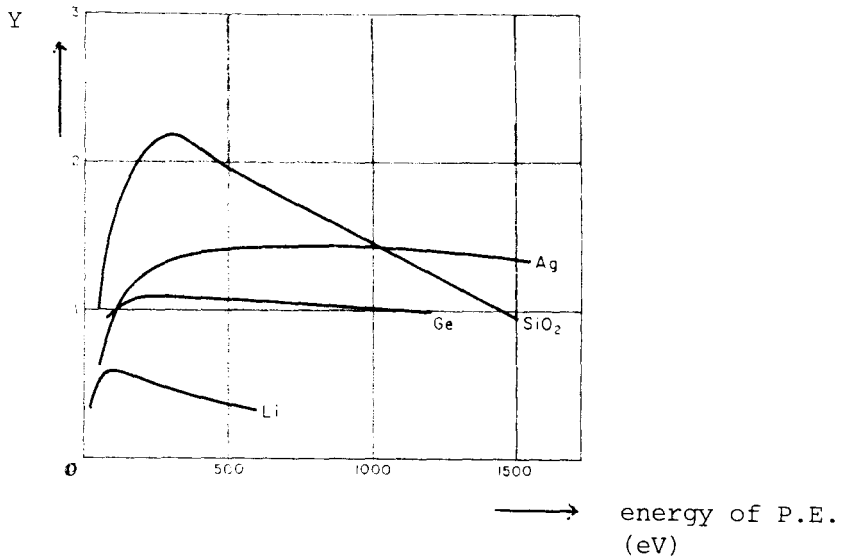

fig. 1.6. : The S.E. yield curves for a number of different materials (GIB66).

If the total yield curves of different materials are normalised with respect to height and position of their maxima, all metals and semiconductors show a remarkable resemblance (GIB66). The total yield of insulators is essentially larger than that for metals and semiconductors. (see 1.2.3.1.) This might be due to the different mechanism of transport of S.E. to the surface in metals and semiconductors, compared to insulators.

Generally it can be said that the yield curve rises for P.E. energies in the range of zero to a few hundred eV. Here it reaches a maximum and then decreases slowly with increasing P.E. energy proportional to $E_{prim}^{-0.8}$ (REI77).

The Y-curve for contaminated and composite surfaces is similar to the one mentioned above, but especially surface contamination has a considerable influence on the magnitude of Y. Whether Y will decrease or increase, depends on the kind of contamination and its homogenity on the surface (see 1.2.3.).

Other factors which effect the magnitude of Y are discussed in paragraph 1.2.3. : The total yield of metals, semiconductors and insulators.

1.2.2. The charging of a target.

Because of a possible difference between the number of incident primary electrons and the number of emitted secondary electrons, charging of the target can occur.
The charging of a target which is exposed to an electron bombardement depends on:

1. the energy of the incident electrons
2. whether the target is a conductor, semiconductor or insulator
3. whether or not the target is connected to earth
4. whether or not the yield of the target at $E_{p\ max}$ reaches a value equal to or larger then 1 somewhere (see fig. 1.7.).

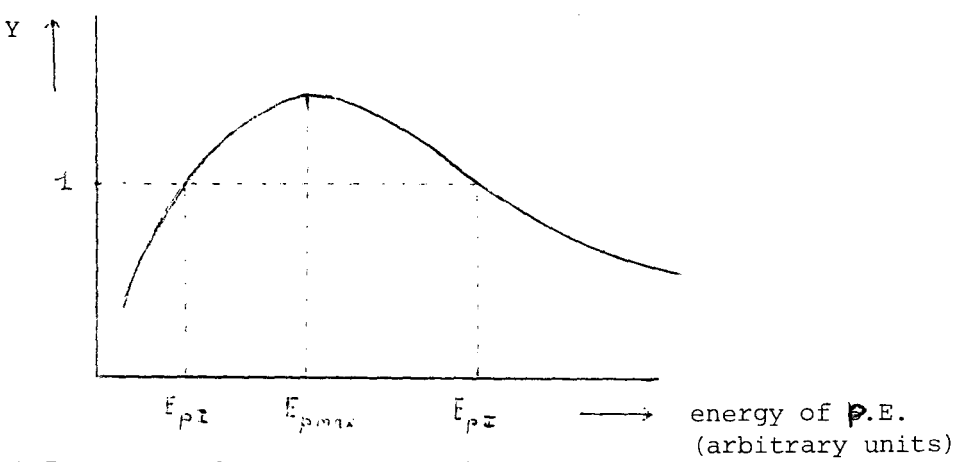

fig. 1.7. : General shape of a yield curve.

In the following all possible combinations will be discussed.

Case A : The target is a conductor or semiconductor and is not connected to earth. (For a good insulator connecting to earth does not differ from not connecting to earth.)
In this case the shape of the yield curve is irrelevant.
No charging will occur because a shortage or an excess of electrons is compensated by a current through the earth line.

Case B : The target, conductor, semiconductor or insulator, is

kept floating and the yield curve is smaller than 1 over the entire energy range.

Now, if a target is kept floating, the charging of it will stop at the moment a balance is reached between the number of emitted S.E. and the number of incident P.E.

As is known, the yield is defined as the number of emitted S.E. divided by the number of incident P.E.
So if Y is smaller than 1 over the entire energy range the target will charge negatively.
The point of balance is obtained when the surface potential of the target reaches the cathode potential.
At that moment, no P.E. can reach the surface anymore so no S.E. are created respectively emitted anymore too.

Case C : The target, conductor, semiconductor or insulator, is kept floating and the yield curve is, over a certain range of energy, larger than 1.

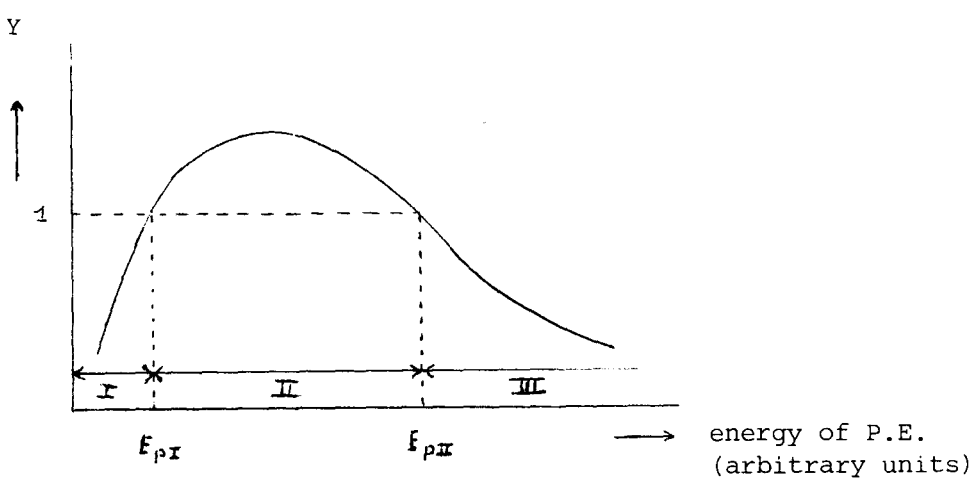

fig. 1.8. : The points where Y=1 are E_{pI} and E_{pII}.
They divide the energy range into three regions of different charging behaviour.

In this case two points of the yield curve play an important role, E_{pI} and E_{pII} , indicated in fig.1.8.
These two points divide the energy range into three regions with different charging behaviour.

Region I : E_p (= energy of the incident primary electrons) is smaller than E_{pI}.

If the P.E. have an energy smaller than E_{pI} , the same thing will happen as indicated in case B. The target will charge negatively until the cathode potential is reached.

Region II : E_{pI} is smaller than E_p which on its turn is smaller than E_{pII}.

If the P.E. have an energy between E_{pI} and E_{pII} , the yield is larger than one. This means that there are more S.E. leaving the surface than P.E. entering it. So the target will charge positively.

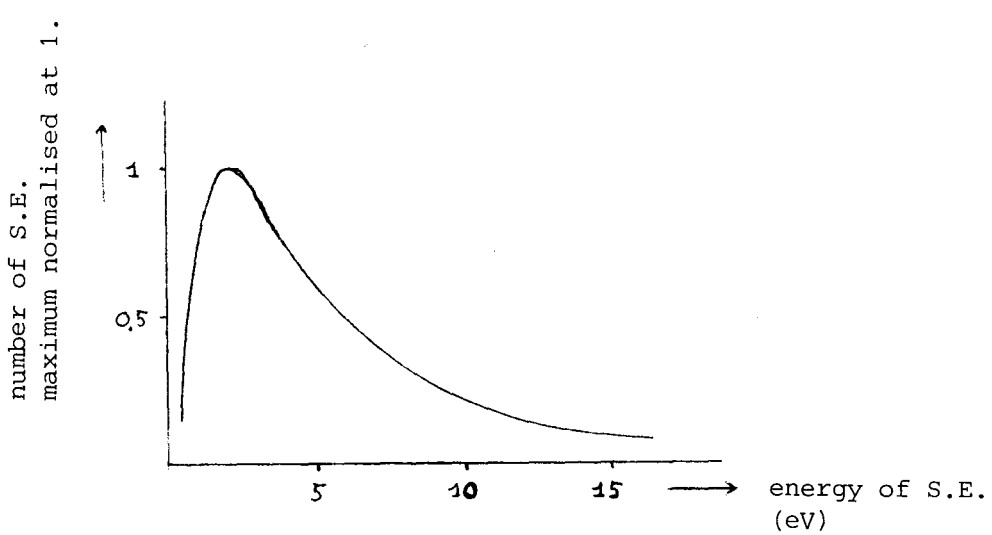

fig. 1.9. : Common energy distribution curve of emitted S.E. for metals (GIB66). For insulators the maximum is generally shifted to a lower value.

To estimate the amount of charging, the energy distribution of the S.E. must be considered.
The energy distribution curve for metals shows a maximum at an energy of about 2 eV.
Generally this maximum lies below 5 eV. So if the surface has a small positive potential, the S.E. with a low energy, are able to escape from the surface, are readily captured by the electric field above the surface and thus cannot contribute to the yield. So a small positive potential of the surface will have a large influence on the number of S.E. that contribute to the yield.

This means that the surface will charge positively a few volts until a balance is reached and the number of incident P.E. equals the number of emitted S.E.

Region III : E_p is larger than E_{pII}.

If the P.E. have an energy larger than E_{pII}, the yield is again smaller than 1.
However the situation is different from that of area I.
The target will charge negatively. This charging will continue until the kinetic energy of the P.E. at the surface equals the value of the E_{pII}.
Then Y is 1 and so a balance is reached. The number of incident P.E. equals the number of emitted S.E.
The surface potential will then have the value:

$$V_{surface} = - (E_{p\ initial} - E_{pII}) / q \qquad (1.1)$$

with: V_{surf} : the surface potential.
$E_{p\ initial}$: the initial energy of the P.E.
E_{pII} : highest energy at which Y is 1. (see fig. 1.8.)
q : elementary charge

The charging results of case C are schematically drawn in fig. 1.10

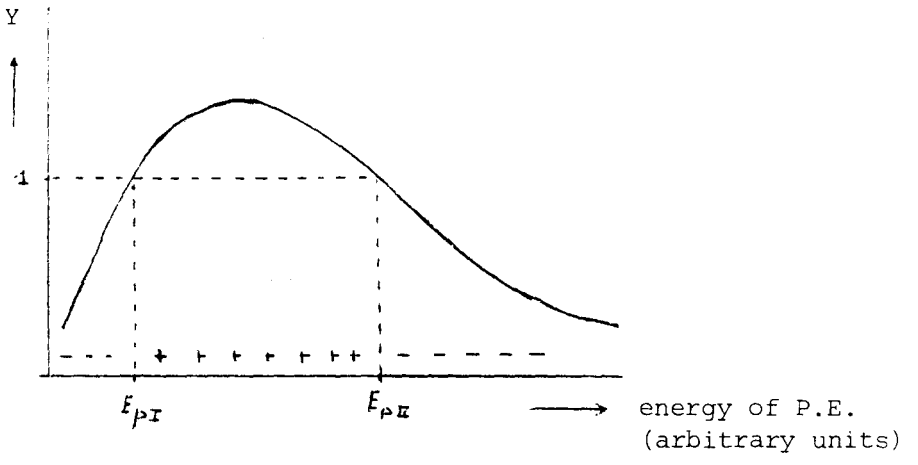

fig. 1.10. : Schematic charging results of case C. The plus and minus symbols indicate the sign of the surface potential with respect to earth.

1.2.3. : The total S.E. yield of metals, semiconductors and insulators.

1.2.3.0. : Introduction.

In this section the total yield of different materials is discussed.

Because metals and semiconductors behave identical with respect to S.E. production, they are further referred to as metals.

Insulators and "metals" have different properties concerning the total yield. These differences are, if extant, described in the following subsections.

Subsection 1.2.3.1. describes a general difference between metals and insulators. Subsection 1.2.3.2. describes the influence of the surface structure on the total yield and subsection 1.2.3.3. does the same for an adsorbed gaslayer.

1.2.3.1. : A general difference between metals and insulators

Although the total yield of S.E. depends strongly on the energy of the incident electrons and on the material of the target, a general difference between "metals" and insulators is immediately apparent from tables 1.1 and 1.2.

Table 1.1. : The secondary emission of insulator mono-crystals (GIB66).

Material	Y_{max}	$E_{p\ max}$ (in eV)	E_{pI} (in eV)	E_{pII} (in eV)
Ge	1.2–1.4	400	—	—
Si	1.1	250	—	—
Se	1.35–1.40	400	—	—
C (Diamond)	2.8	750	—	—
NaCl	14	1.2 k	10	—
NaBr	24	1.8 k	—	—
KCl	12	—	10	—
KI	10.5	1.6 k	12	—
KBr	12–14.7	1.8 k	10	—
MgO	23	1.2 k	—	—
SiO_2 (Quartz)	2.1–2.9	400–440	50	2.3 k
Mica	2.4–2.75	325	25–40	3.0 k
$Al_2O_3 \cdot MgO$ (Spinel)	3.6	450	<300	>3.5 k
$Al_2O_3 \cdot Cr_2O_3$ (Ruby)	3.8	900	<300	>3.5 k
GaAs	1.1	350	—	—
InSb	1.15	700	—	—

Table 1.2. : The secondary electron emission of pure metals (GIB66).

Atomic No.	Metal	Y_{max}	$E_{p\ max}$ (in eV)	E_{pI} (in eV)	E_{pII} (in eV)
3	Li	0.52	100	—	—
4	Be	0.5	200	—	—
5	B	1.2	150	50	550
6	C				
	(Graphite)	1.02	300	250	350
	(Aquadag)	0.75	350	—	—
	(Soot)	0.45	500	—	—
11	Na	0.82	300	—	—
12	Mg	0.97	275	—	—
13	Al	0.97	300	—	—
14	Si	1.1	250	120	520
19	K	0.53	175	—	—
20	Ca	0.6	200	—	—
22	Ti	0.9	280	—	—
24	Cr	1.10	400	250	900
25	Mn	1.35	200	50	750
26	Fe	1.3	200	120	1400
27	Co	1.35	500	120	>1500
28	Ni	1.35	450	140	1100
29	Cu	1.28	600	200	>1500
30	Zn	1.4	800	150	2800
31	Ga	1.08	600	300	1000
32	Ge	1.08	400	100	800
37	Rb	0.9	300	—	—
38	Sr	0.72	400	—	—
40	Zr	1.1	350	190	600
41	Nb (Cb)	1.2	350	150	1100
42	Mo	1.2	350	140	1100
46	Pd	1.65	550	90	>1500
47	Ag	1.56	800	140	>2000
48	Cd	1.59	800	<100	>4000
49	In	1.4	500	<100	>4000
50	Sn	1.35	500	200	>1400
51	Sb	1.3	600	250	2000
55	Cs	0.72	400	—	—
56	Ba	0.85	300	—	—
73	Ta	1.25	600	275	1500
74	W	1.35	650	250	1500
78	Pt	1.5	750	350	3000
79	Au	1.79	1000	150	>4000
80	Hg	1.3	600	350	>1200
81	Tl	1.4	800	<100	>4000
82	Pb	1.1	500	250	1000
83	Bi	1.15	550	180	1600
90	Th	1.1	800	—	—

Namely the maximum total yield of S.E. of metals is generally smaller than that of insulators.
According to Gibbons (GIB66) this can be explained as follows:

For insulators the minimum energy that can be lost by free electrons is equal to the energy difference between the top of the valence band and the bottom of the conduction band, the bandgap. This gap is roughly 5 eV or higher.
The only way by which these free electrons may lose energy, once they have an energy equal to the energy gap, is by collision with lattice defects and through electron-phonon interactions.

In a monocrystal the number of collisions with lattice defects will be small. Although the number of electron-phonon interactions may be large, the amount of energy exchanged in such an interaction is very small.
So free electrons in mono-crystalline insulators with an energy of only a few eV, will have a high probability of travelling large distances in the crystal.
If the workfunction is smaller than the energy difference between the conduction band and the valence band, these electrons have a large probability to be emitted from the surface.

For metals everything is a bit different. In a metal there are many free and losely bound electrons with which the S.E. can collide, involving the transfer of large or small amounts of energy. A thermal equilibrium arises between the produced S.E. and the free and losely bound electrons in the lattice. So the mean free path of S.E. in a metal will be smaller than in insulators and the median energy will be smaller too. So if the workfunctions of metals differ not too much from those of insulators, the foregoing differences can explain the general difference between the total yield of S.E. of metals and insulators.

1.2.3.2. : The influence of the surface structure on the total yield.

Different faces of a monocrystal have often different values for the workfunction. Therefore one may expect a different yield of S.E. for different crystal faces and indeed this is found (KNO39).

But other factors play a more important role, e.i. the state of order and the roughness of the surface.

Suhrmann and Kundt (SUH43) showed that S.E. emission in the ordered state of Cu, Ag and Au is greater than in the disordered state by as much as 30 percent.

The differences are greatest in the region of $E_{p\ max}$ (the energy of the P.E. where Y has it maximum).

However Woolridge (WOO40) showed that for Cu_3Ag these changes were less than 1 percent. So the changes strongly depend on the material under observation.

The surface roughness has an even greater influence on the total yield. This is illustrated in table 1.3.

Table 1.3. : The difference of Y_{max} for rough and smooth surfaces (GIB66).

Type of surface	Y_{rough}	Y_{smooth}	$\frac{Y_{rough}}{Y_{smooth}}$
Nickel, polished electrolytically	1.29	1.35	0.96
Nickel, aluminized	1.38	1.35	1.06
Nickel, blackened in methane	1.0	1.35	0.77
Nickel, sintered	0.99	1.35	0.77
Nickel, covered with TiO_2	0.83	1.35	0.61
Tantalum, rolled	1.27	1.25	1.02
Tantalum dust sintered on tantalum	1.04	1.25	0.83
Reduced tungsten trioxide on tungsten	0.57	1.45	0.39
Thermally processed tantalum pentoxide on tantalum	0.66	1.25	0.53
Zirconium powder sintered on molybdenum	0.58	1.1	0.44
Titanium dioxide sintered on molybdenum	0.66	0.9	0.75
Tungsten, electrolytically matted	1.56	1.45	1.06
Soot deposited from flame[42]	0.48	1.05	0.46
Soot settled from alcohol suspension[42]	0.7	1.05	0.67

According to Bruining (BRU38-1,2; GIB61) one might expect a lower S.E. emission and thus a smaller Y_{max} for rough surfaces compared to smooth ones.
This is due to the formation of microscopic cavities which act as miniature Faraday cages (see fig. 1.10), out of which the S.E. cannot escape.

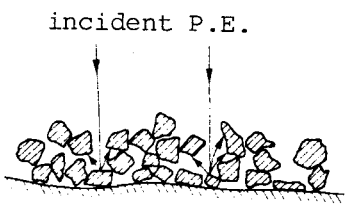

fig. 1.11. : The influence of a rough surface on S.E. emission, according to Bruining.

However, from table 1.3 it can readily be seen that this point of vieuw is not generally true.
Here some values of Y_{rough} / Y_{smooth} are larger than 1.
Other aspects of the surface structure must also be considered if one wants to say something about the influence of roughness on the total yield.
For instance the kind of roughness has to be considered like the size and sharpness of the grains and/or the edges and the electrical contact between the grains.

So although the roughness may have a large influence on the total yield, it is hard to say what the final effect will be.

1.2.3.3. : The influence of an adsorbed gaslayer on the total yield.

As already mentioned in 1.2.3.2., a reduction of the workfunction of the surface leads to an increase of Y of the material.

The workfunction of a metal can be reduced by adsorption of ions of an electropositive metal. A particular example is shown in fig. 1.12.

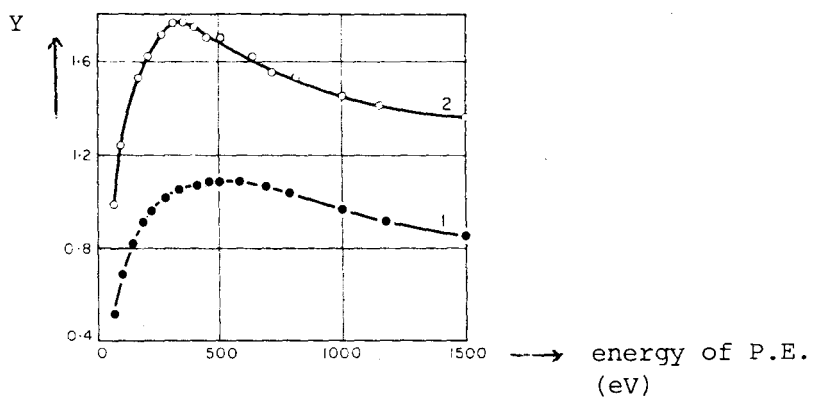

fig. 1.12. : The secondary emission of a germanium target,
1. before adsorption of caesium vapour
2. after adsorption of caesium vapour (GIB66)

In the same way the workfunction of a surface may be lowered by the adsorption of a gaslayer.
A particular example of this is the adsorption of an oxygen layer. For most materials Y increases if an oxygen layer is adsorbed on their surface.
If in the case of adsorption of oxygen oxides are formed, even a much higher increase of Y is observed (GIB66).
An exception to this rule is tungsten. Here an increase of the workfunction is measured if a monolayer of oxygen is adsorbed. The increase of the workfunction is due to the formation of an electrical double layer. (See also par. 1.2.5. : some special properties of insulators).

Generally it can be said, that if an adsorbed gaslayer changes the workfunction, the total yield of the target is changed. The lower the workfunction, the higher the total yield.

p = adsorption coefficient of the material

x, i = are explained in fig. 1.13.

k = proportional konstant

This seems in reasonable agreement with the experimental data (BRU38-1,2 and GIB66).

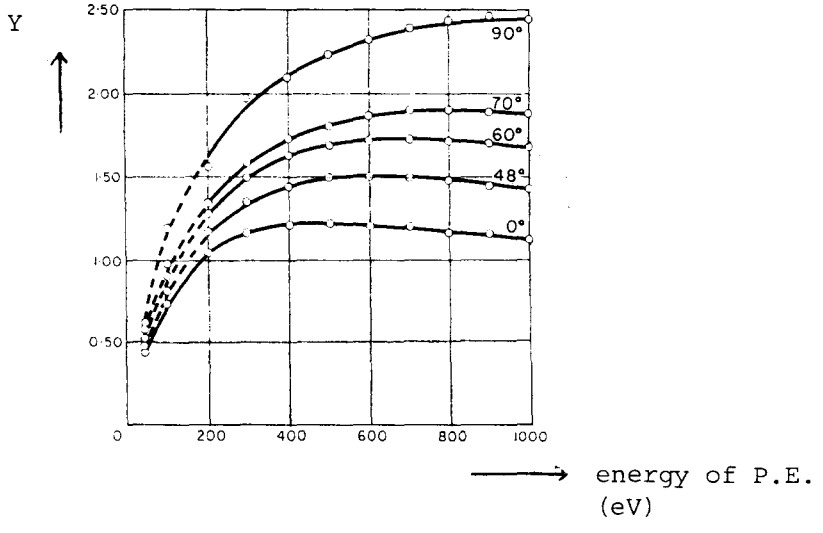

fig. 1.14. : The S.E. emission of Ni as a function of the angle of incidence (BRU38-1,2 and GIB 66).

For rough surfaces the variation of Y with the angle of incidence is found to be very small, in accordance with what could be expected, since the angle of incidence is poorly defined on such a surface (BRU38-1,2 and GIB66).
The angular distribution of the emitted S.E. hardly varies with the angle of incidence of the P.E..
This is shown in fig. 1.16. a,b and c (JON51).

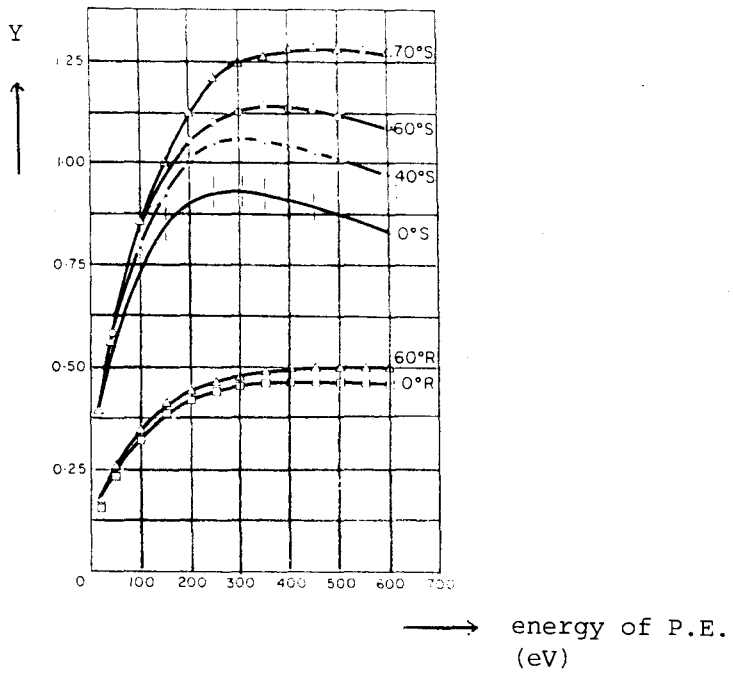

fig. 1.15. : The total S.E. emission as a function of the energy of the P.E. for various angles of incidence:
S: smooth target (nickel carbide)
R: rough target (soot).

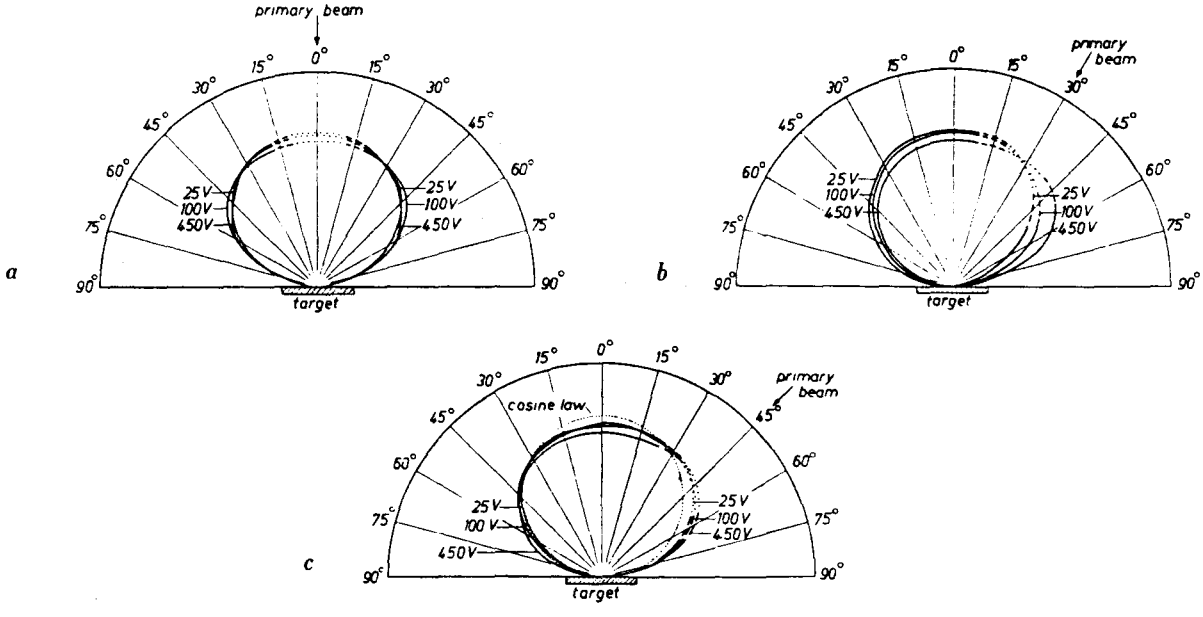

fig. 1.16. : The angular distribution of S.E. of nickel for different accelerating voltages of the P.E. and different angles of incidence (arrow) (JON51).
Note : these curves are not meant to give the absolute distribution so all curves are enclosing an equal area for better comparison.

1.2.5. : Some special properties of insulators.

Proper measurements of the secondary electron emission of insulators always have been a problem.
This is originated by all kinds of charging effects.

In early years problems arose when the angular dependence of Y was measured. It was thought that a so called critical angle of incidence existed at which the yield dropped to a very much lower value by increasing angle. This effect was not found for metals (KOL37). However it turned out to be a charging effect that could be eliminated if careful precautions were taken (KOL56).

A second charging effect in which an insulating layer plays an important role, is the Malter effect.
This effect was first observed by Malter in 1936. A surface which shows this Malter effect, contains essentially three layers.

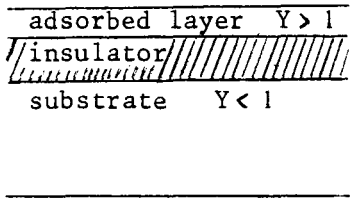

fig. 1.17. : The necessary surface composition for the Malter effect.

These are shown in fig. 1.17. : a layer with a total yield larger than 1, an insulating layer and a third layer (which can be the substrate) with a total yield smaller than one.
Mostly the toplayer is an adsorbed layer. The insulating layer must be able to withstand the strong electrostatic field.

However, to obtain the Malter effect the two upperlayers must de as thin as to let the incident primary electrons reach the substrate.

Now the upperlayer will, under electron bombardement, charge positively with respect to the substrate. This is possible because of the insulating layer between them.
A strong electric field will be formed over the insulating layer. This will, if a certain field strength is reached induce field emission of electrons from the negative bulk to the surface layer.
These field emitted electrons partly produce S.E. in the insulator and the surface, partly are emitted from the surface and, partly, are absorbed by the insulator and the adsorbed layer.
Finally a balance establishes between the electrical field strength created by the incident P.E. and the number of electrons which are emitted due to field emission.

A third charging effect which especially occurs at insulators was firstly measured by Hintenberger in 1939.
For P.E. energies just a little above E_{pI} he at first measured a positive charging of the surface as could be expected.
But after some time the surface potential sank, first slowly, later more quickly, to the kathode potential.
This effect did not occur at energies of P.E. much larger than E_{pI} , but still with a Y larger than 1.
Hintenberger explained the first part of these results as follows.
At first the surface charges positively because Y is greater than 1. But the P.E. which penetrate the insulator will stay captured a certain distance below the surface and will form a negative space charge inside the insulator. Firstly this effect will stimulate the emission of electrons. But because of the space charge the P.E. will lose their energy quicker and penetrate less deep.

So the area with the negative space charge grows into the direction of the surface. This causes a smaller yield because of a smaller area where the S.E. can be created.
If on the long run the yield becomes smaller than one, the surface potential will have to drop to the kathode potential.
Hintenberger does not explain why this effect does not occur for energies which are much larger than E_{pI} but still have a yield larger than 1.

The fourth effect has nothing to do with charging, but with the influence of impurities in the insulator crystal on the total yield.

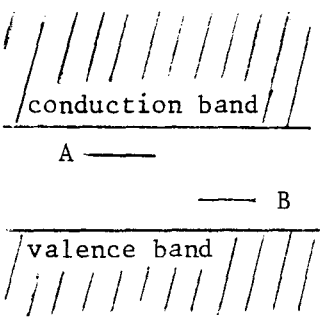

fig. 1.18. : Energy levels between the bottom of the conduction band and the top of the valence band can have a large influence upon the Y-value.

Impurities in a monocrystaline insulator can lead to additional energy levels between the bottom of the conduction band and the top of the valence band.
It is clear that they can have a large influence on the S.E. yield. Whether the additional levels will decrease or increase the Y-value depends on whether they act as donor or acceptor levels.
For instance, if A (see fig. 1.18.) acts as a donor level this

could lead to more electrons in the conduction band and thus to more electron - electron interactions with a possible recapturing at level A. So this would lead to less S.E..

Another possibility would be segration of the impurities to the surface. This could lead to a decrease of the workfunction and thus an increase of the number of emitted S.E..

Both an increase and a decrease of the total yield is found by several authors (KOL56). To what extend the impurities themselves act as emission centres is still unknown.

1.3. : The model of the electron beam etching process.

With the knowledge of the former paragraphs of this chapter, a model for the beam etchprocess can be made.

As is known electrons themselves do not etch a surface, they merely charge or melt it.
An adsorbed gaslayer is needed. This gas must be choosen well. It must not etch the substrate without activation by electrons, especially the S.E. (see par. 1.1.).
The interaction with the S.E. will lead to the formation of ions which have to be directed towards the surface. (see par. 1.2.).
On interaction with S.E. the adsorbed gasmolecules will form ions. Since the adsorbed gasmolecules have certain, although very small, dimensions, most of the time the ions are created a couple of Å above the surface, so they must be directed towards it. Ions can be accelerated in an electric field so it depends on the charge of the ions and the potential of the surface whether or not the ions are accelerated towards the surface.
If the target is a metal or a semiconductor, this potential can be applied with an external supply. This gives, for conductors, the possibility to choose the accelerating voltage at which the total yield Y has its maximum value. If the conductor is only grounded no charging of the surface occurs and it then depends on the initial direction of the impulse of the ion if and where the ion will reach the surface. However, if the surface is kept floating or we deal with insulators, charging may occur due to electron bombardement. The sign of the charging decides about the direction of the acceleration of the ions and thus whether local and directed etching will occur or no etching at all.

So, to obtain directive etching charging of the surface is needed. As is shown in section 1.2.2.,charging of a floating

target with P.E. always leads to a balance between the number of incident P.E. and the number of emitted S.E.. Whether finally the number of S.E. emitted per second will be equal to 0 or equal to the number of P.E. incident per second depends two things (see par. 1.2.2.), namely the initial energy of the incident P.E. with respect to the surface and the yield curve.

For materials with a yield curve which is over the entire energy range smaller than 1, the point of balance is obtained as soon as no P.E. are able to reach the surface anymore and thus no S.E. are produced and emitted anymore.

However, as is discussed in par. 1.2.4., an adsorbed gaslayer may lower the workfunction of the surface so the yield curve of the system may be increased to or above the Y = 1 level in a certain range.

Assume a surface plus adsorbed gaslayer has over a certain P.E. energy range a yield larger than 1.

This means a balance is possible at which the number of S.E. equals the number incident P.E. and is not 0 (see par. 1.2.2.).

The initial energy of the P.E. with respect to the surface must then be choosen larger then E_{pI}.

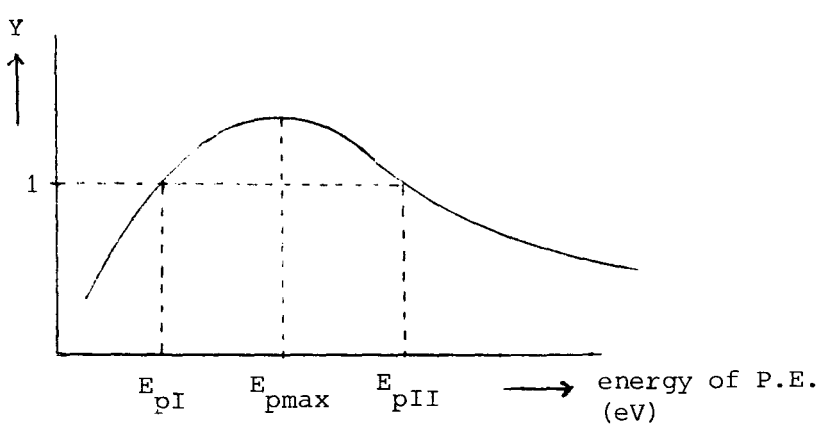

fig. 1.19. : A general yield curve.

Assume further that the adsorbed gaslayer is able to produce ions on interaction with S.E. and that these ions can etch the surface. In that case the choice of the initial energy of the P.E. depends on which, positive or negative, ions etch the surface.

If positive ions etch the surface, then the initial energy of the P.E. must be choosen larger than E_{pII} to establish a negative surface charge.
Else the energy must be choosen somewhere between E_{pI} and E_{pII} and so much larger than E_{pI} as to avoid the "Hintenberger-effect" (see par. 1.2.4.).

If negative ions are used to etch, a positive surface charge is required. This charge induces (see par. 1.2.2.) a shifting of the S.E. energy distribution to the left (see fig. 1.20.).

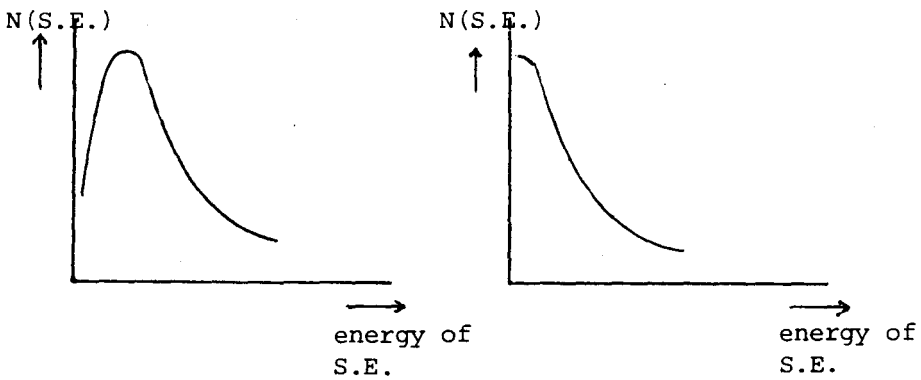

fig. 1.20. : The effect of positive charging on the S.E. energy distribution.

This means a lowering of the median energy of the S.E..

On negative charging of the surface, the energy distribution curve of the S.E. will shift to the right. This means an increase in the median energy.

It must be noticed that these effects are of a macroscopic scale. Microscopic (just above the surface) the influence of the charging of the surface on the S.E. emission is probably not present.

There is another interesting phenomenon to note as is pointed out in section 1.2.5.. For insulators there exists a critical angle of incidence if no special care is taken of the charging effects (see fig. 1.21.).

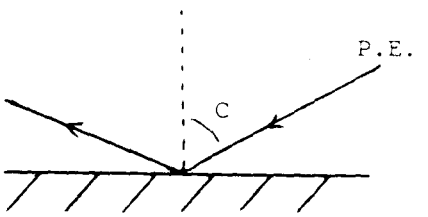

fig. 1.21. : Critical angle of incidence due to the charging of the surface of an insulator.

If the angle of incidence becomes larger than c, no S.E. are emitted anymore, because no P.E. can reach the surface.
Now look at fig. 1.21.

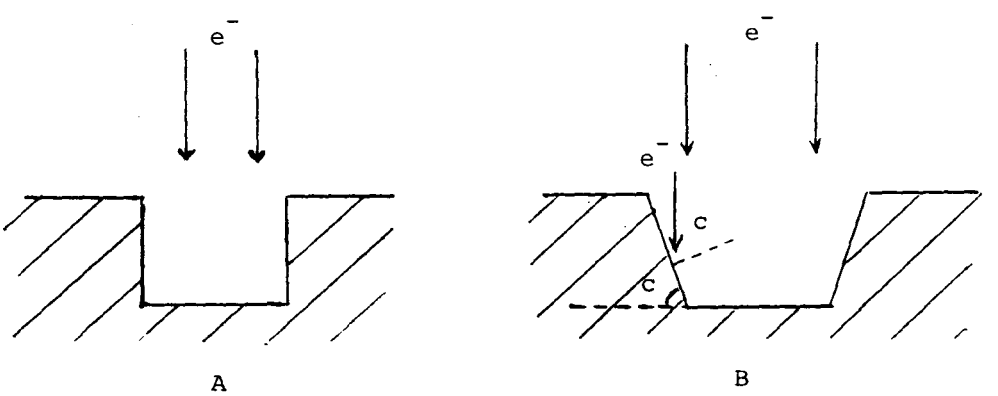

fig. 1.22. : A : Ideal case of etching
B : What might occur due to the critical angle of incidence

The ideal case of etching is shown in figure 1.22.A.
Steep walls perpendicular to the bottom of the etched hole.
In fig. 1.22.B is shown what may occur due to the existence of the critical angle c.
The walls will have an angle of approximately c to the bottom. Approximately c because other effects can play a role too, for instance S.E. emitted at the bottom may activate the adsorbed gasmolecules on the walls.

1.4. : The etching of silicondioxide.

1.4.0. : Introduction.

Because we are especially interested in the etching of silicondioxide, the demands for the etchgas are treated referring to silicondioxide. For other materials the same kind of considerations have to be made.
First the choice of the etchgas is treated in 1.4.1.
Then the way of adsorption of the chosen gas on silicondioxide is treated in 1.4.2.

1.4.1. : The choice of the etchgas.

As will be clear from the former paragraphs, the etchgas molecules must have some specific properties.

The first is that these molecules must contain one or more parts (atoms) which on their own must be able to form stable and gaseous products with the surface atoms.
Possible stable gaseous products are, in our case, SiF_4, $SiOF_2$ and $SiCl_4$. This means that candidate etchgas molecules must contain F and/or Cl atoms.

A second demand is that the molecule must adsorb on the surface and even at an elevated temperature, that might be due to the incident electron beam, stick there long enough to complete the process.

Considering these two demands, trifluoroacetic acid, CF_3COOH, was choosen. It contains three fluorine atoms that can react with the silicondioxide surface and a -COOH group, of which it is generally known that it adsorbs well on surfaces.
From measurements done at the Philips Research Laboratories it is known that this gas even at 100 degrees Celcius adsorbs very well (more than 90 % coverage) at SiO_2.
How the CF_3COOH (further referred to as T.F.A.A.) is adsorbed on the silicondioxide surface is discussed in the next section.

1.4.2. : The method of adsorption of trifluoroacetic acid on silicondioxide.

Two essentially different methods of adsorption can be distinguished : physical adsorption and chemical adsorption.

Physical adsorption is due to Van der Waals forces and dipole interactions. Adsorption energies up to 0,4 eV/molecule (BRO83) are possible. (To convert eV/molecule to kJ/mol multiply with 96,36.) So these molecules are weakly bound to the surface.

An estimation of the adsorption energy of T.F.A.A. on SiO_2 can be given with a simple model for the physical adsorption process called Miedema's model (BRO83). However this model does not take into account the mutual interaction of the molecules due to their permanent dipoles, nor the interaction of these dipole molecules with the surface. It only deals with the interactions due to Van der Waals forces.
In the case of T.F.A.A. Miedema's model must be corrected for these interactions.

According to Miedema the adsorption energy of material A on material B is

$$E_{ads\ A,B} = -2.(1-s).E^{\frac{1}{2}}_{surf\ A}.\ E^{\frac{1}{2}}_{surf\ B} \qquad (1.5)$$

with : $E_{ads\ A,B}$ = adsorption energy of A on B
s = strangeness parameter
$E_{surf\ A}$ = surface energy of A

The surface energy can be estimated with the heat of sublimation. (BRO83)

$$\Delta H_{subl\ A} = 6N_0.\ E_{surf\ A}.(V_{mol}/N_0)^{2/3} \qquad (1.6)$$

with : N_0 = number of Avogadro
$E_{surf\ A}$ = surface energy of A
$\Delta H_{subl\ A}$ = sublimation energy of A
V_{mol} = molar volume of A

which gives :

$$E_{surf\ A} = \Delta H_{subl\ A} / b.(V_{mol})^{-2/3} \qquad (1.7)$$

with : $b = 6N_0^{1/3} = 51.10^7 \quad (mol^{-1/3})$

So, for the surface energy of T.F.A.A. we obtain with (1.7) and appendix I :

$$E_{surf\ T.F.A.A.} = 42.2 \quad (mJ/m^2) \qquad (1.8)$$

This leads, with (1.8), (1.5), appendix I and the strangeness parameter s assumed 0, to an uncorrected adsorption energy of :

$$E_{ads\ T.F.A.A.,SiO_2} = -260 \quad (mJ/m^2) \qquad (1.9)$$

$$= -0.2 \quad (eV/molecule) \qquad (1.10)$$

This value of-0.2 eV/molecule is obtained if we assume that on every SiO_2 surface molecule a T.F.A.A. molecule is adsorbed (s=0).

The correction for the dipole interaction consists of two parts. The first part originates from the interaction of the dipoles with the surface, the second part originates from the mutual interaction of the adsorbed molecules.

The interaction of the dipoles with the surface can be seen as the interaction due to the creation of mirror charges in the surface. As soon as a charged particle appears above a surface, conductible or not, there are always enough free charge carriers to create an equipotential plane at the surface-vacuüm interface. This means that the mirrorcharge method can be applied to estimate the dipole - surface interaction.

The model used for the calculation of the dipole interactions is shown in figure 1.23.

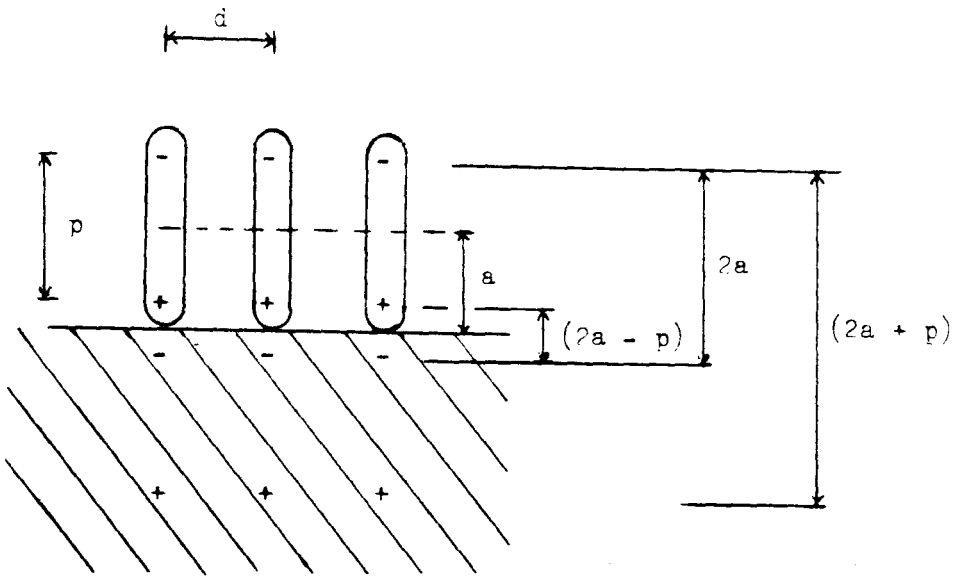

fig. 1.23. : The model used for the calculation of the correction of the dipole interaction.

As is seen, an adsorbed dipole layer is supposed. Further the interaction with 4 nearest neighbours is taken into account. Considering the large uncertainty of some quantities in this model, it is not useful to calculate interactions with dipoles at larger distances than the 4 nearest neighbours.

The potential energy of the molecule due to the interaction of the dipole with its mirror charges can be written as :

$$U_{mir.ch.} = U_{1,mir.ch.} + 4.U_{n.n.mir.ch.} \qquad (1.11)$$

with : $U_{mir.ch.}$ = potential energy due to the interaction with the mirror charges.

$U_{1,mir.ch.}$ = potential energy due to the interaction of the dipole with its own mirror charge.

$U_{n.n.mir.ch.}$ = potential energy due to the interaction of the dipole with the mirror charge of its nearest neighbours.

Assume, for simplicity, that the classical calculation method is valid, then :

$$U_{l,mir.ch.} = (-q^2/4\pi\varepsilon_c).((1/(2a-p)) + (1/(2a+p))) + \\ +(2q^2/4\pi\varepsilon_o).(1/2a) \quad (1.12)$$

$$= (-q^2/4\pi\varepsilon_c).(p^2/a(4a^2-p^2)) \quad (1.13)$$

and

$$U_{n.n.mir.ch.} = (q^2/4\pi\varepsilon_o).(2/\sqrt{4a^2+d^2} - 1/\sqrt{(2a-p)^2+d^2} + \\ -1/\sqrt{(2a+p)^2+d^2}) \quad (1.14)$$

with : a,d and p = as explained in figure 1.22.

So, finally :

$$U_{mir.ch.} = (q^2/4\pi\varepsilon_o).(-p^2/a(4a^2-p^2) + 8/\sqrt{4a^2+d^2} + \\ 4/\sqrt{(2a-p)^2+d^2} - 4/\sqrt{(2a+p)^2+d^2}) \quad (1.15)$$

The potential energy of the dipole molecule due to the interaction with a nearest neighbour is :

$$U_{dip.n.n.} = 2.(q^2/4\pi\varepsilon_o).(1/d - 1/\sqrt{p^2+d^2}) \quad (1.16)$$

So with 4 nearest neighbours we get :

$$U_{dip.n.n.tot.} = (2q^2/4\pi\varepsilon_o).(1/d - 1/\sqrt{p^2+d^2}) \quad (1.17)$$

So the total potential energy of a dipole molecule when it is adsorbed at a surface is :

$$U_{dip.} = U_{mir.ch.} + U_{dip.n.n.tot.} \quad (1.18)$$

$$= (q^2/4\pi\varepsilon_o).(-p^2/a(4a^2-p^2) - 8/\sqrt{4a^2+d^2} + \\ - 4/\sqrt{(2a-p)^2+d^2} - 4/\sqrt{(2a+p)^2+d^2}) + \\ + (2q^2/4\pi\varepsilon_o).(1/d - 1/\sqrt{p^2+d^2}) \quad (1.20)$$

The dipole moment of the molecule can be explained in two different ways.

The first is a separation of two elementary charges of opposite sign at equal distance from the centre of the molecule. For T.F.A.A. (with data from appendix I) this would mean a distance between the two charges of 0.48 Å.

The second is a small permanent shift of the electron cloud of the molecule due to a stronger elektronaffinity of certain parts of the molecule. If the complicated structure of T.F.A.A. is neglected and only two centres of charge (one positive and one negative) are thought to exist at 0.5 Å from the ends of the molecule and if the molecule is thought of as a rod with a length of 3.97 Å (see appendix I), the value of the small charges is $2.56.10^{-20}$ C.

If the first point of view is followed we obtain :

with a = 1.99 Å $q = 1.6.10^{-19}$ C

d = 3.5 Å

p = 0.48 Å

$U_{mir.ch.}$ = - 0.17 eV

$U_{dip.n.n.tot.}$ = + 0.30 eV

--------- +

$U_{dip.}$ = + 0.13 eV

If the second point of vieuw is followed we obtain :

with a = 1.99 Å $q = 2.56.10^{-20}$ C

d = 3.5 Å

p = 2.97 Å

$U_{mir.ch.}$ = - 0.27 eV

$U_{dip.n.n.tot.}$ = + 0.20 eV

--------- +

$U_{dip.}$ = - 0.07 eV

Now if the adsorption energy according to the Miedema model (- 0,2 (eV)) is corrected with these values we obtain respectively - 0,07 (eV) and - 0,27 (eV).

Conclusion :

If chemical adsorption occurs, the molecules are chemically bound to the surface by covalent and/or ionic bonds. Possibly they are split when they adsorb. Adsorption energies of 0,4 to 7 (eV/molecule) are possible (BRO83), so the molecules are strongly bound to the surface.

Although nothing was found in literature on the adsorption of T.F.A.A. on silicondioxide, some general remarks can be made. It is known from the adsorption of acetic acid on ZnO (BOW82) that the -COOH group adsorbs on the ZnO surface. First the double bound oxygen atom adsorbs. This leads to the weakening of the O-H bond. This, on its turn, leads to the splitting of the hydrogen atom from the O-H bond under the formation of a O-H bond with the surface oxygen and the binding of the second oxygen atom of the acetic acid molecule on the surface in such a way that both oxygen atoms are bound in a similar way.

It is thought that such a way of adsorption could also be possible for trifluoroacetic acid on silicondioxide. Such a structure is shown in figure 1.24 and is called a resonant bond.

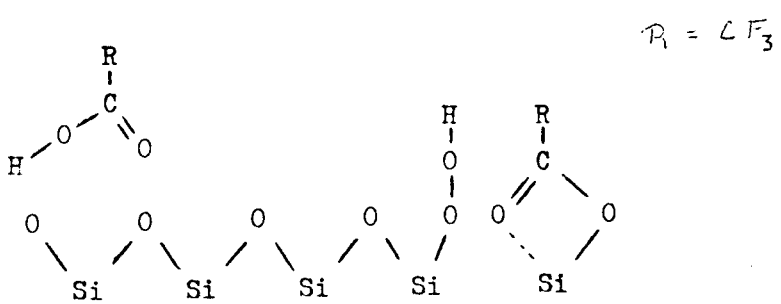

fig. 1.24. : A possible way of chemical adsorption of T.F.A.A. on SiO_2.

The way of adsorption pointed out above is quite complicated. For the binding of T.F.A.A. on silicondioxide a more simple structure can be given as is shown in figure 1.25.

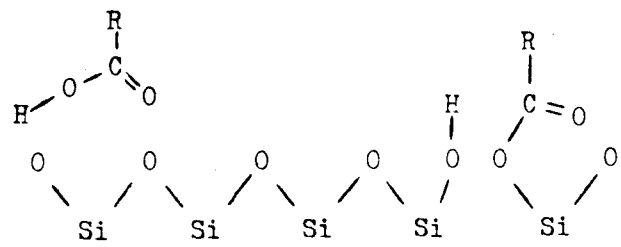

fig. 1.25. : A simple way of chemical adsorption of T.F.A.A. on SiO_2.

Note that in the foregoing figures the oriëntation of the molecules with respect to the SiO_2 surface was not taken into account. Further it must be noted that for the way of adsorption as is shown in figure 1.25 the enthalpy of the reaction will be very small. In both ways of binding all kinds of factors could play an important role, like the elektronaffinity of the Si and the C atom and a possible relaxation of the tension of the O-Si-O-Si bond.

Concluding to this section it can be stated that physical adsorption is possible according to the corrected Miedema model. Whether and how chemical adsorption will occur is hard to say. Even a two stage process might be possible, first physical adsorption followed by chemical adsorption.

Chapter 2 : The experimental arrangements.

2.0. : Introduction.

This chapter is divided into four parts : the vacuum system, the electrical system, the target mounting and the preparation of the target.
These subjects are described in the following paragraphs.
In figure 2.1. a schematic drawing of the total set up is given.

2.1. : The vacuum system.

The vacuum system has been described and tested by J. v.d. Pol in 1980 (POL80).

The main parts are :

- the rotary pump, a D30A (Leybold Hereaus) with a pump speed of 3,06 l/s. This pump is used to create a preliminary vacuum down to 2.10^{-2} Torr.
- the oildiffusion pump, type Diff250 (Balzers), with a pump speed of 130 l/s. On top of this pump a permanently freon cooled baffle is mounted. A second baffle, on top of the freon baffle, can be cooled with liquid nitrogen. The pumping speed above the baffles is unknown.
  This pump is used to create the end vacuum of 2.10^{-6} Torr.
  This pressure is reached after about 4 hours of pumping.
- two Al_2O_3 oil vapour traps. They serve as a trap for the oil vapours of the rotary pump which pass the water cooled baffle just above this pump.
- the massaspectrometer, a Topatron B (Leybold Hereaus).
  With this instrument the residual gas can be analyzed.
  Although it has an inaccuracy of 10% in the mass, an indication of the components of the residual gas is available.
  A typical spectrum is shown in figure 2.2.

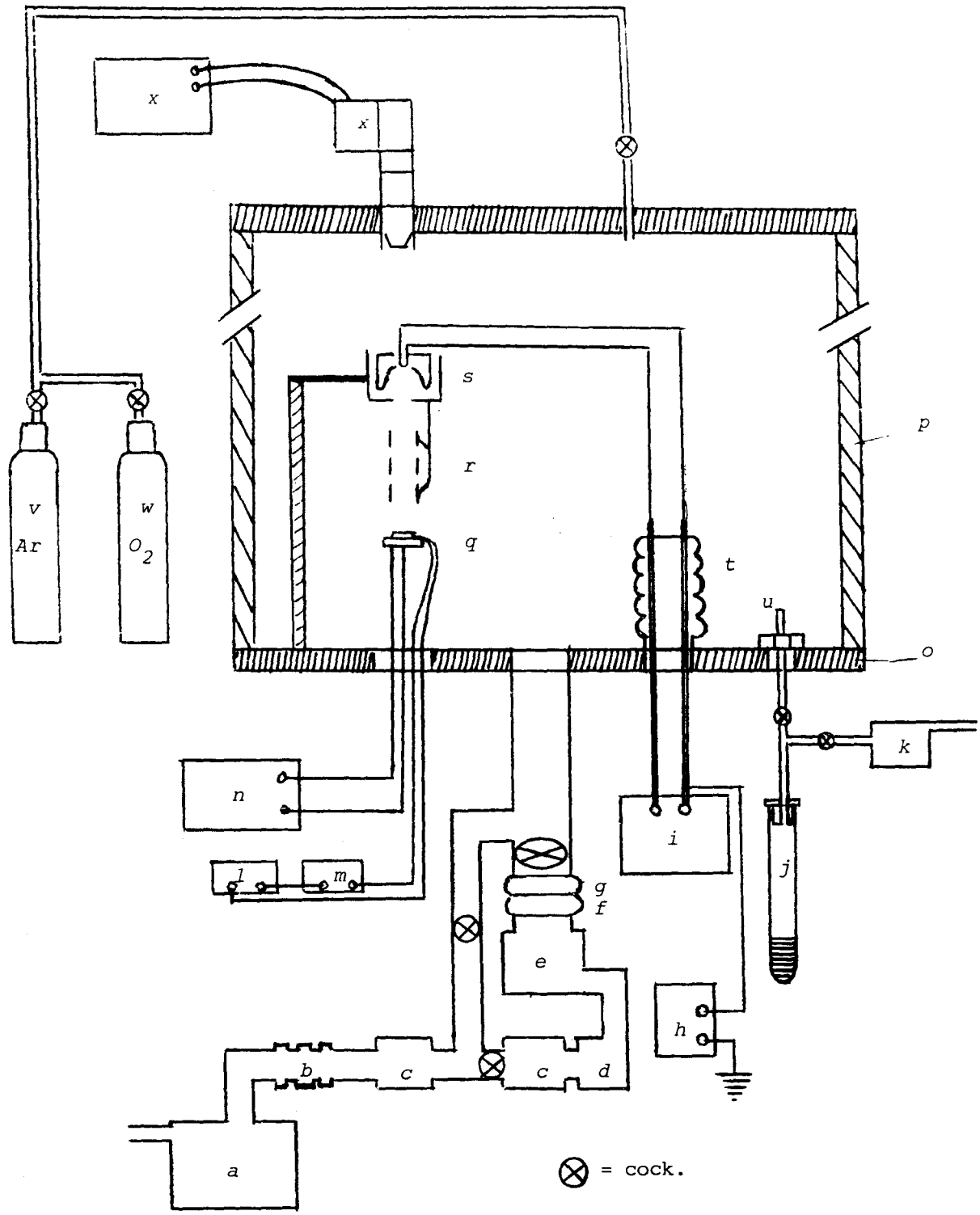

fig. 2.1. : A schematic drawing of the experimental arrangements.

For the explanation of the used synbols see next page.

List of symbols of figure 2.1.

a : *rotary pump for preliminary vacuum.*

b : *water baffle.*

c : *aluminium oxide baffle.*

d : *buffer of oil diffusion pump.*

e : *oil diffusion pump.*

f : *freon cooled baffle.*

g : *liquid nitrogen cooled baffle.*

h : *high voltage supply for electron gun.*

i : *current supply for electron gun filament.*

j : *glass bulb with etchgas liquid.*

k : *rotary pump for preliminary vacuum of glassbulb j.*

l : *microvolt meter.*

m : *microvolt supply.*

n : *current supply for heater of target holder.*

o : *bottom flange of vacuum system.*

p : *glass cylinder of vacuum system.*

q : *target holder.*

r : *Einzellens.*

s : *electron gun.*

t : *high voltage feedthrough.*

u : *etchgas inlet.*

v : *gascontainer with Ar.*

w : *gascontainer with* O_2.

x : *mass spectrometer.*

Specifications :

- pressure : 1.5 10^{-6} Torr
- emmision current of the Topatron : 300 µA.
- scan time : 2 minutes.

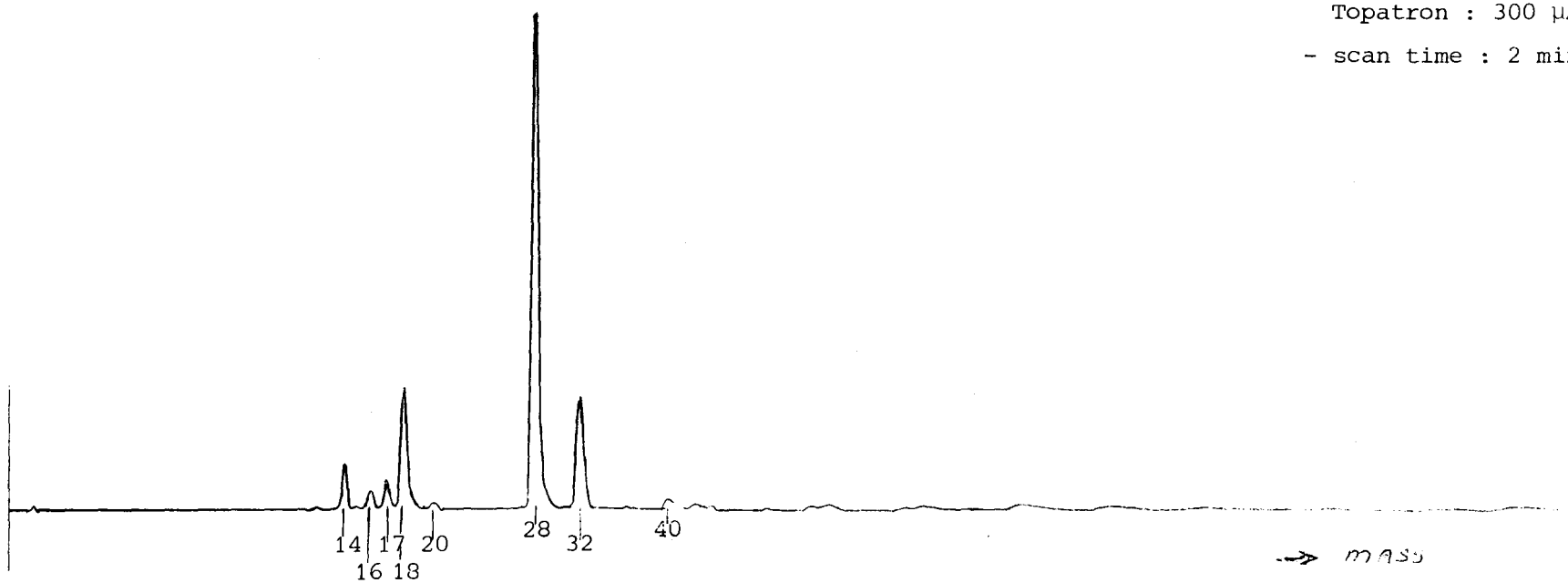

fig. 2.2. : A typical residual gas spectrum of the vacuum system, measured with the topatron.

2.2. : The electrical system.

The electron gun is a VeB-6 gun (Pierce type, Veeco). It is designed for the production of high power electron beams up to 6 kW at an accelerating voltage of 20 kV and 3 kW at 11 or 15 kV accelerating voltage. It originally was used for the evaporation of silicon.

The above given specification did not meet the desired ones : adjustable accelerating voltage up to 4 kV and adjustable beam currents up to 1 mA. So, some changes were required.

The regulation of the accelerating voltage was firstly acquired with a 3 fase variac, placed in the supply line of the high voltage transformer. Although the accelerating voltage could be controlled this way, the beam power regulation stayed insufficient in the lower regions. So another electrical operating system of the gun was needed. The ultimate system is given in figure 2.3.

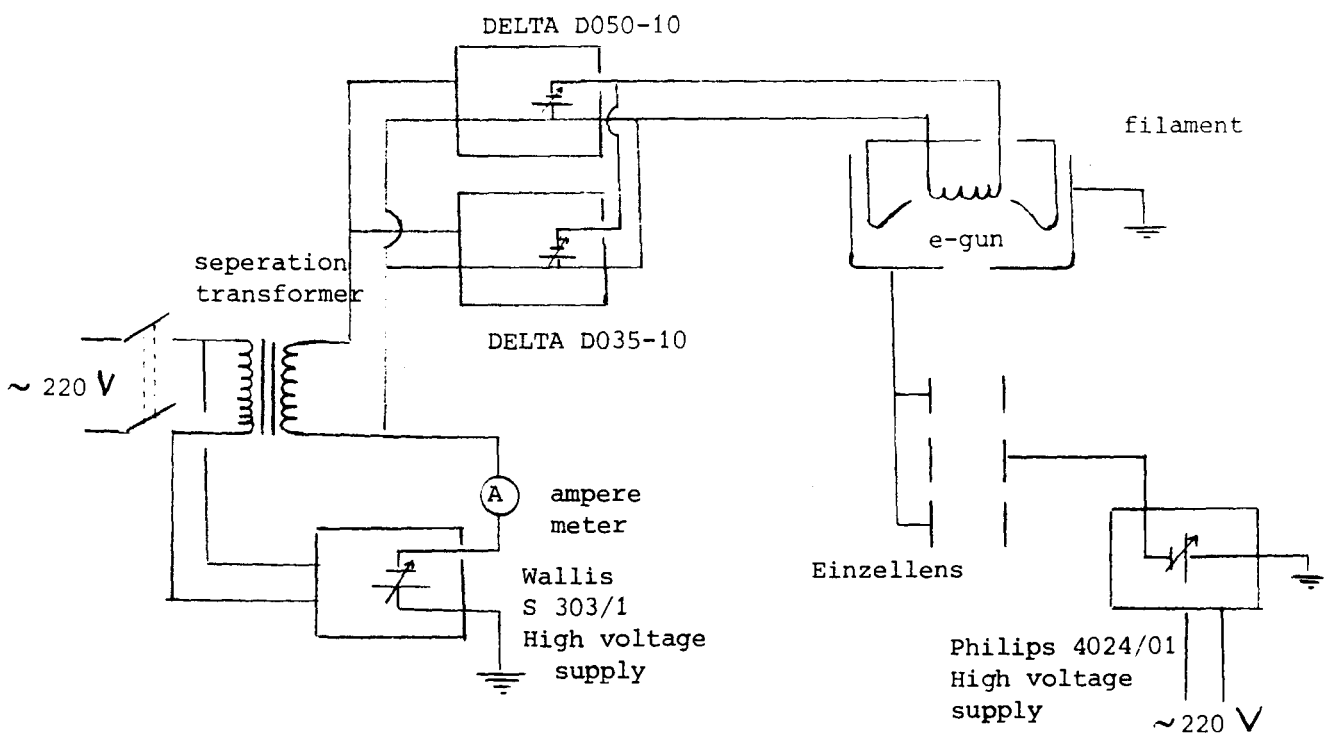

fig. 2.3. : Schematical drawing of the electrical system for the operation of the electron gun.

With this system the accelerating voltage can be adjusted from 0 to 15 kV and the beamcurrent can be regulated with the parallel coupled power supplies, which here serve as current supplies for the filament. The current emitted from the filament can be measured with the amperemeter A.
The spot diameter of the electron beam can be optimized with the Einzellens. A spot diameter of 2 mm and a beamcurrent of 1 mA is obtainable. (Spot diameter determined with the eye and fluorescent screen.) Although the spotdiameter is very large for Integrated Circuit apllications it is small enough for the experiments.

2.3. : The wafer mounting.

The target holder is drawn in detail in figure 2.4.

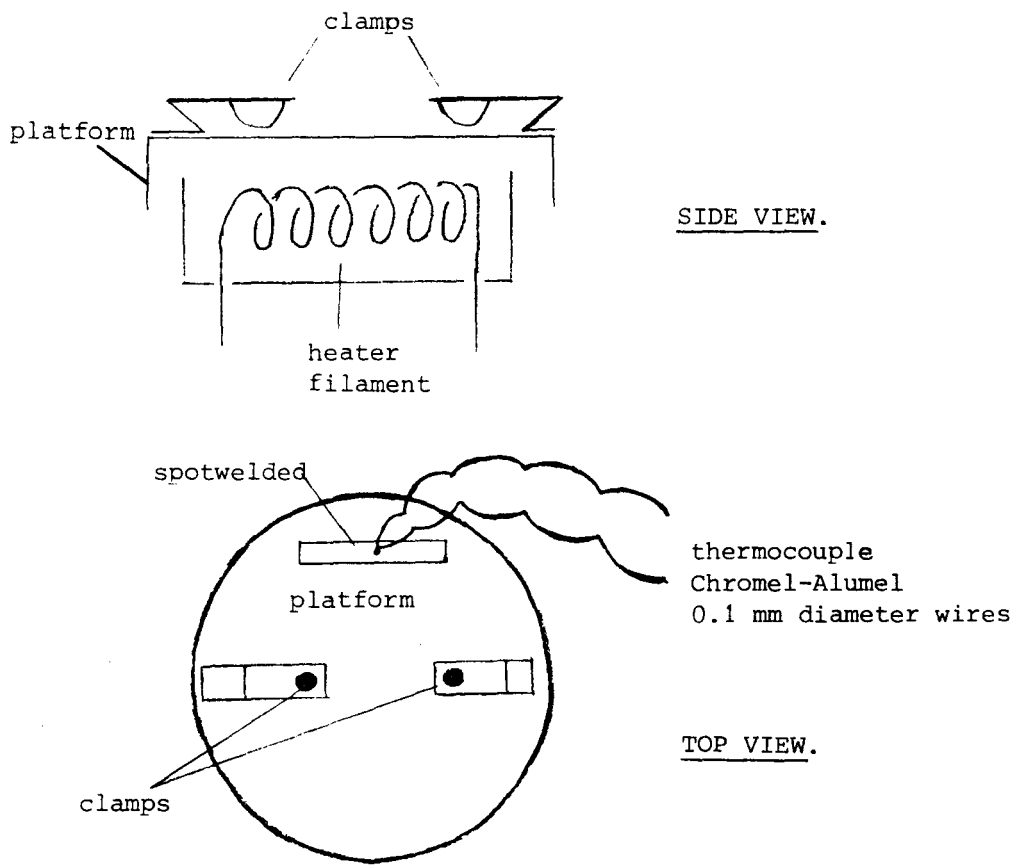

fig. 2.4. : The target holder.

The target holder is a modified heater. The modification consist of clamps and a thermocouple.
The heater can reach temperatures up to 1000 degrees Celcius. It is only used at 450 degrees Celcius. The temperature of the top of the heater is measured with a Chromel - Alumel thermocouple with a wire diameter of 0,1 mm.
The thermocouple is spotwelded on top of the heater and the temperature is measured with the so called "cold weld temperature compensation" method. The pressing of the target on the top of the heater realises a sufficient thermal contact.

2.5. : The preparation of the target.

The monocrystalline silicon targets all had a thick surface oxide layer (± 3200 to 4600 Å).
Two different types of silicon were used as substrate.
The first was a p-type silicon with a typical resistance of 3 Ωm and an oxide layer of about 4600 Å thick. This layer was formed by chemical vapour deposition.
The second type was an n-type silicon substrate with a typical resistance of 3 to 5 Ωm and an oxide layer of about 3200 Å thick. This oxide layer was thermally grown.
In both cases the crystal face of the substrate was the <100> face.

From the wafers smaller pieces of 10 by 10 mm were cut. On these pieces aluminium strips were applied to the surface by vapour deposition. The result is shown in figure 2.5.

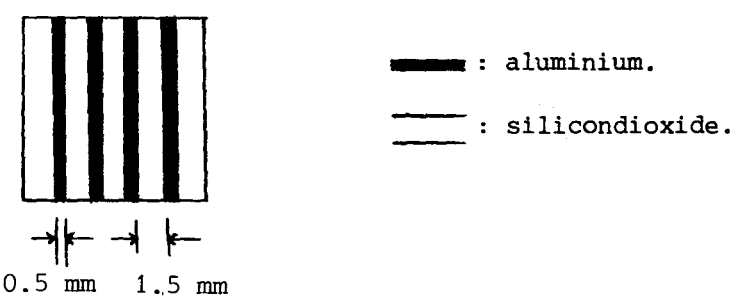

fig. 2.5. : The surface of the preparate after the vapour deposition of the aluminium strips.

Before the target was exposed to the etchgas and the electron beam (see paragraph 1.3.) in the same vacuum it was heated to 450 °C for 1 hour in an atmosphere of 2.10^{-4} Torr oxygen. After cooling of the wafer the etchprocess was started. During the etchprocess the oxygen pressure was 2.10^{-5} Torr and the T.F.A.A. pressure was 2.10^{-4} Torr. The extra inlet of O_2 was done because earlier experiments showed that this reduced the deposition of carbon on the surface.

Chapter 3 : Results and discussion.

3.0. : Introduction.

In this chapter the results of the measurements are given. However, firstly some problems, which had an influence on the outcome of the experiments, are discussed in paragraph 3.1. In section 3.1.1. the problem with the stability of the electron beam is discussed. Section 3.1.2. discusses the determination of the beam current during the experiments. Section 3.1.3. deals with the determination of the etched volume.
With the knowledge from these sections the measurements can be discussed.
In paragraph 3.2. the dependence of the etching process on the accelerating voltage is treated. In paragraph 3.3. the dependence of the etchrate on the total amount of incident charge is treated. Finally in paragraph 3.4. The efficiency of the process is discussed.

3.1. : Some problems during the experiments.

3.1.1. : Problems with the stability of the electron beam.

The main problem with the electron gun during the experiments was the instability of the beam current. There are two sources for this instability namely the pressure variations during the experiments and the instability of the current supply of the filament of the electron gun.

The gun was operated at a pressure of 10^{-4} Torr. Small pressure variations (a factor 2) resulted in large beam current variations. These pressure variations were probably induced by an unstable gasflow of T.F.A.A. into the vacuum system.

This unstable gasflow on its turn can be due to a changing of the evaporation velocity of T.F.A.A. which can be originated by many things for instance a changing of the temperature of the T.F.A.A. liquid, a reaction of the T.F.A.A. with the water vapour in the system or a reaction of the T.F.A.A. with the different materials of the gass supply system followed by a dillution of the liquid.

The reaction of T.F.A.A. with the materials of the gass supply system was often noticed. At the front end of the supply system, where the glass bulb with T.F.A.A. was connected, the T.F.A.A. vapour could freely react with the Viton O-rings and stainless steel. Once, a dilluted solution of T.F.A.A. was analysed and nearly all components of stainless steel were found in it. In order of decreasing quantity Fe, Cr, Ni, Zn, Mn, Mg and Co were detected.
In figure 3.1. a mass spectrum of fresh T.F.A.A. is shown.
Figure 3.2. shows a spectrum of dilluted T.F.A.A.

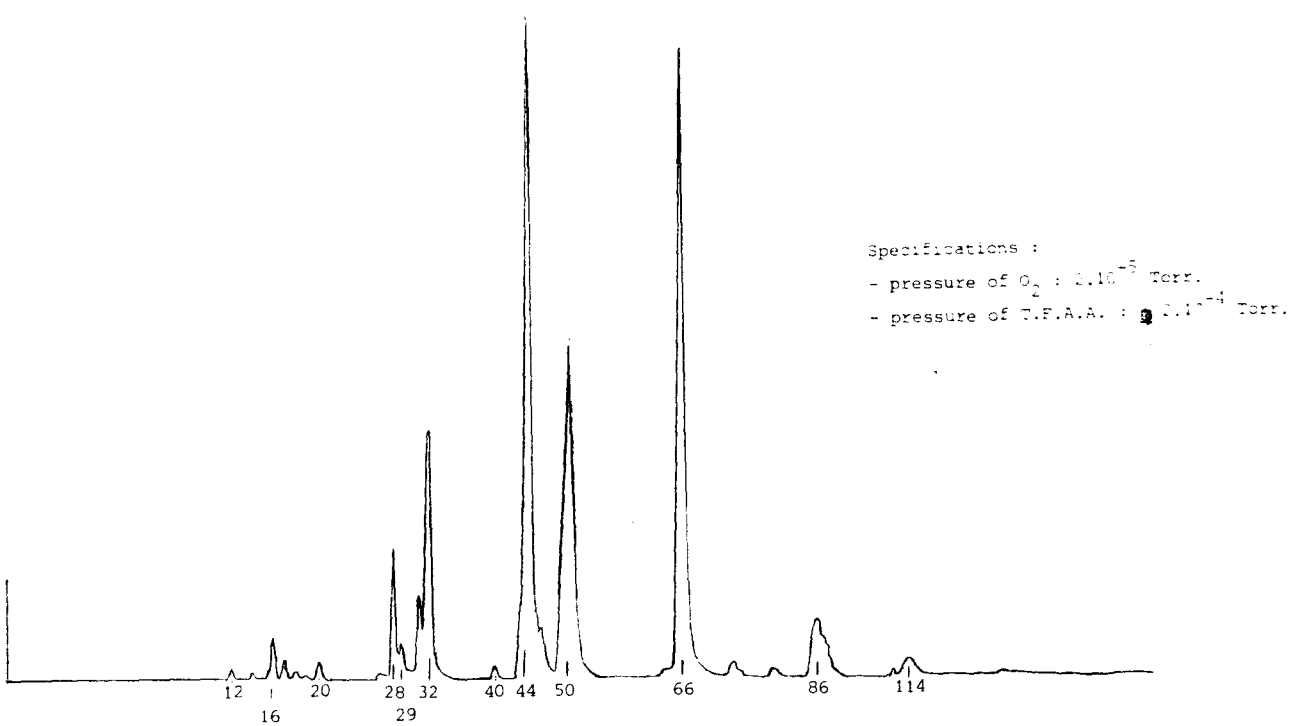

fig. 3.1. : A mass spectrum of fresh T.F.A.A.

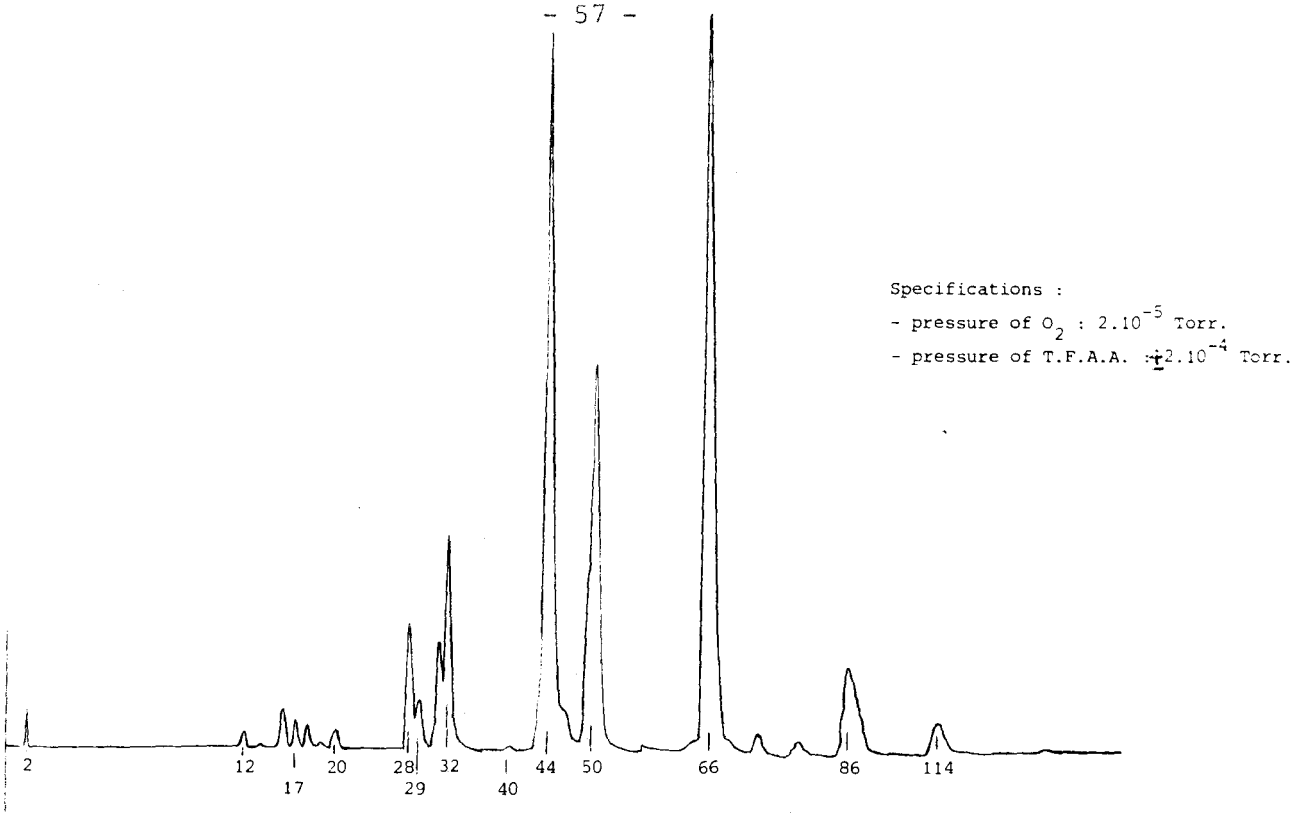

fig. 3.2. : A mass spectrum of dilluted T.F.A.A.

Because the H_2 peak is the only significant difference, no further attention was paid to it.

The instability of the current supply of the filament of the electron gun was partly a temperature effect and partly an effect due to the parallel connection of two power supplies. From the specifications of these power supplies (Delta Elektronica D 035-10 and D 050-10) it follows that parallel connection could freely be done. This parallel connection was necessary because currents of about 13 A were needed to operate the electron gun.

The temperature effect was slightly reduced by the use of a blower for extra cooling power of the power supplies. The parallel coupling instability could partly be reduced by operating the two supplies at about the same current. However, still changes of sometimes 0.2 A occured which induced large changes in the beam current. In figure 3.3-1 a typical course of the emitted current during the etching process is displayed. In figure 3.3-2 the dependence of the emitted current on the filament current is given.

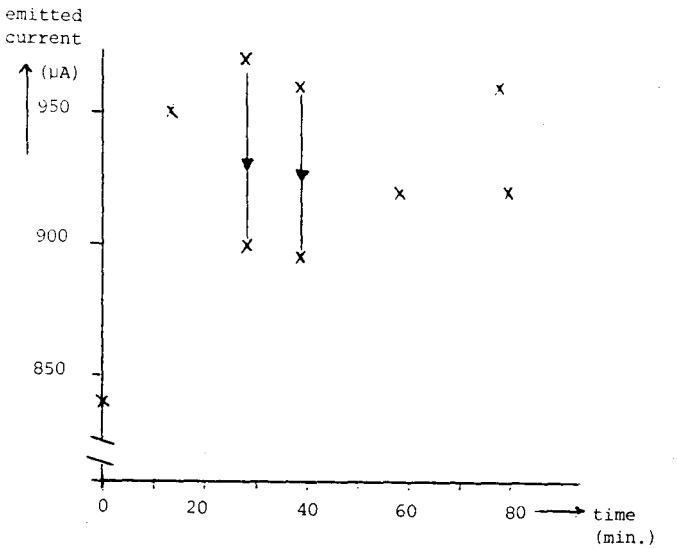

fig. 3.3-1 : A typical course of the emitted current during the etchprocess. The arrow indicates the direction of executed adjustments.

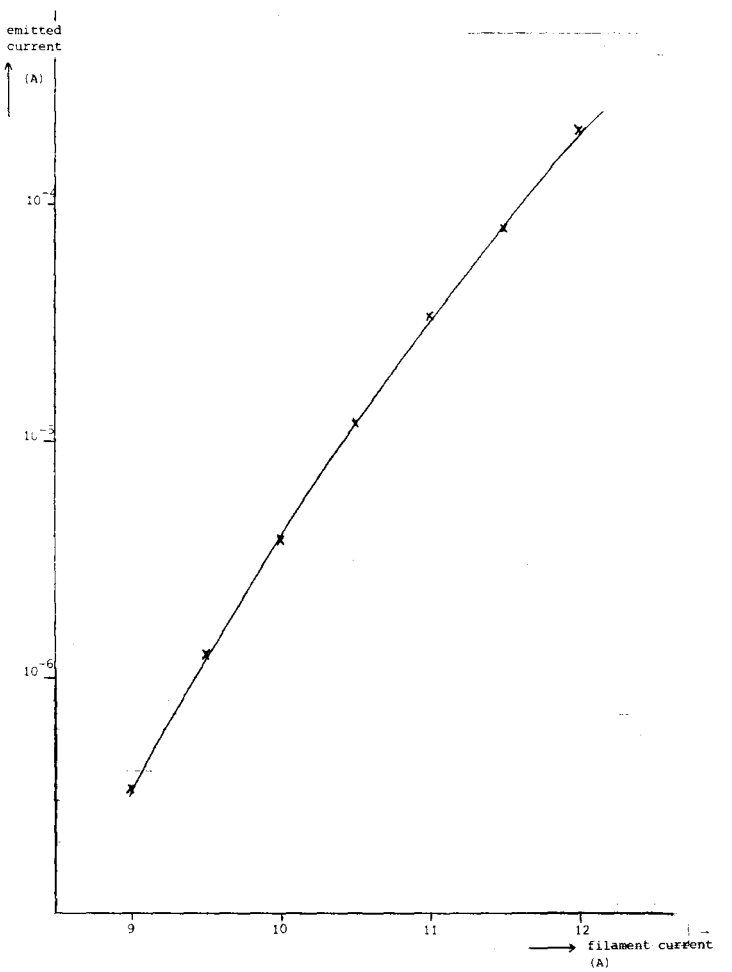

fig. 3.3-2 : The dependence of the emitted current on the filament current.

3.1.2. : The determination of the beam current.

As is shown in chapter two the emitted current from the filament is measured with an ampere meter. This ampere meter is placed in the electric wiring from the high voltage supply to the current supply of the filament. The value obtained in this way has to be corrected for the current losses on the kathode and the Einzellens to obtain the beam current on the target.

It was tried to calibrate the readings of the ampere meter by direct current measurements with a wire netting with known throughput. The experimental arrangement for this measurement is shown in figure 3.4.

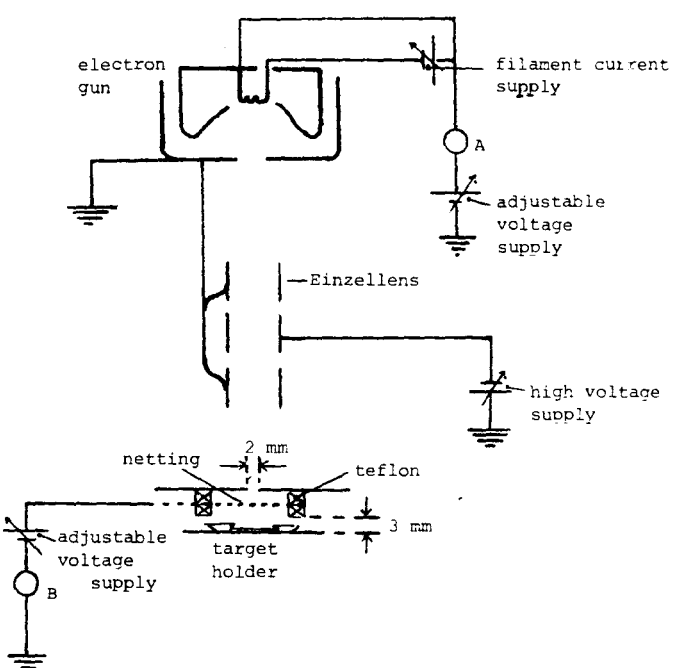

fig. 3.4. : Experimental arrangements for the direct measurement of the beam current.

However, it turned out that the wire netting itself produced so much S.E. that no reliable measurements were possible. This can be seen in figure 3.5. where the effect of a positive offset voltage on the wire netting on the current measurements are shown. Beside this, the by the wire netting emitted S.E. influenced the etching process in such a way that no etching occured anymore.

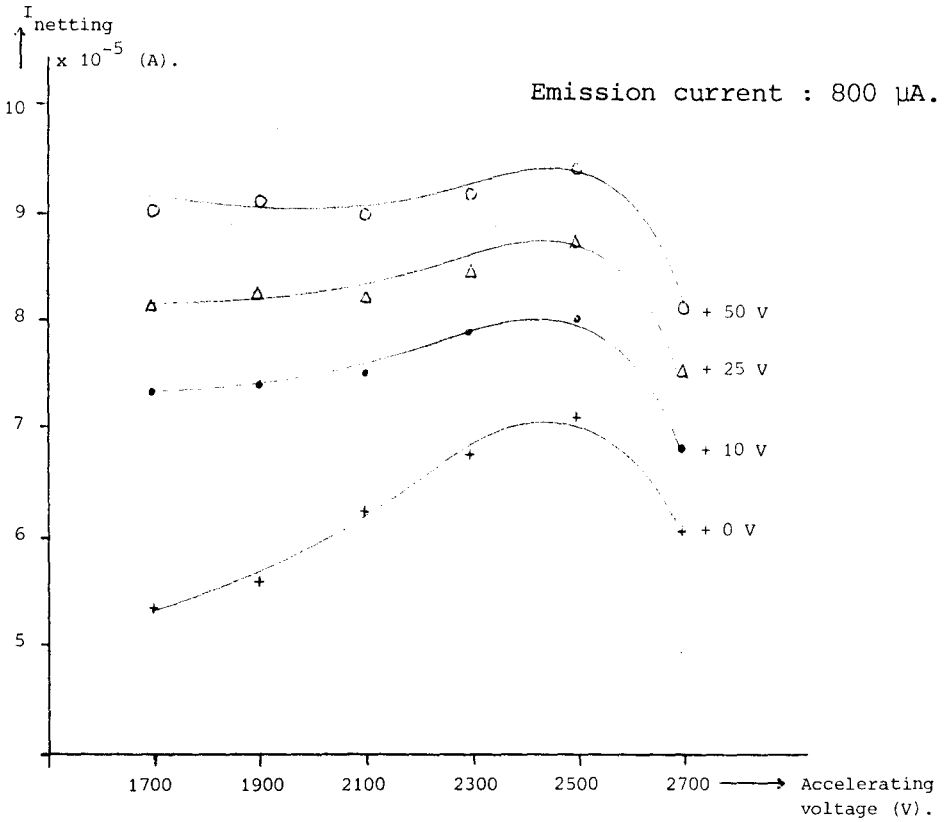

fig. 3.5. : The measurements of the beam current with the wire netting and the influence of a positive offset voltage put on the netting.

So it was decided to calibrate the readings of the ampere meter with the aid of a Faraday cup. The experimental arrangements for this are shown in figure 3.6.

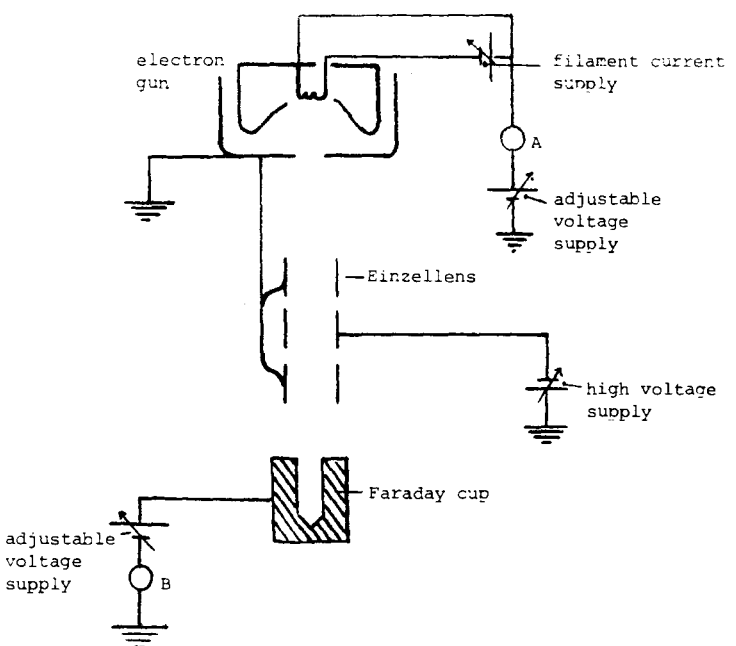

fig 3.6. : The experimental arrangements for the measuments of the beam current with a Faraday cup.

Here the effect of the S.E. produced by the cup was measured too. When a positive voltage of 100 V was put on the cup the current readings increased less then 3 %. So the S.E. had no significant influence on this measurement. The callibration factors, for the determination of the beam current from the emitted current are displayed in table 3.1..

Table 3.1. : The calibration factors for the determination of the beam current incident on the target from the current emitted by the filament.

Accelerating Voltage (V).	Calibration Factor.
1700	0.85 ± 0.01
1800	0.81 ± 0.01
1900	0.80 ± 0.01
2000	0.80 ± 0.01
2100	0.81 ± 0.01
2200	0.82 ± 0.01
2300	0.83 ± 0.01
2400	0.82 ± 0.01
2500	0.82 ± 0.01

Further, because of the instability of the emitted current during the process, the current was measured about every 10 minutes during the process. The process itself took mostly about 90 minutes. The currents given in table 3.3. (see par. 3.2.) is the weighted mean value of these measurements.

3.1.3. : The determination of the etchrate.

Aluminium strips were evaporated on to the surface (see chapter 2) to obtain sharp edges between an etched zone and, after the removal of the aluminium strips, a non etched zone. These sharp edges were necessary for proper measurements with a Tallystep (available at the C.T.D.,T.H.E.).

A Tallystep is an apparatus which is able to measure height differences as small as 20 Å over small distances. However, the depth of the etched hole can also be measured with the aid of a simple light microscope and a colour table (see appendix II) for SiO_2. The apparent colour, when looked at the SiO_2 layer from above, is a measure for the SiO_2 layer. This is only true if the SiO_2 layer is on top of a reflecting and colourless substrate.

The first measurement was done with both the Tallystep and the microscope. These results differed less than 50 Å. At higher beam currents difficulties appeared with the removal of the aluminium strips. Thus, further on, the depth of the etched holes were measured with the light microscope and the colour table.

Because the beam diameter is unknown and probably not constant during all experiments, the etched depth is not a proper measure for the etchrate. The etched volume should be a better quantity.

The volume of the etched hole is determined as follows (see also figures 3.7. and 3.8.).

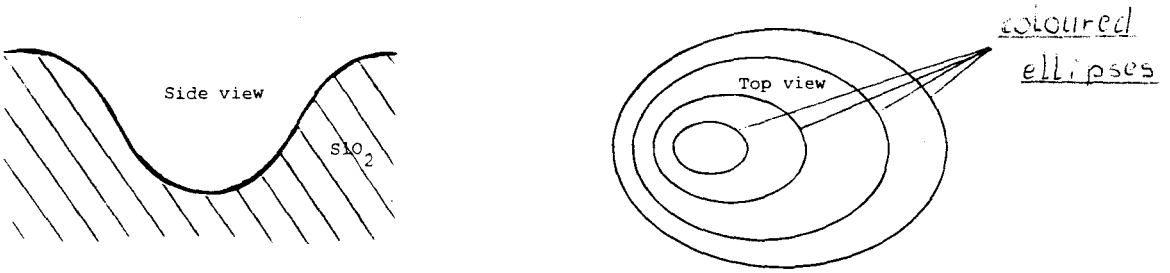

fig. 3.7. : Side view and top view of an etched hole.

Looked upon from above, the bottom of the etched hole is surrounded by coloured ellipses. These coloured ellipses originate from the variation of the thickness of the SiO_2 layer with respect to the Si substrate (see figure 3.7.).

For easiness we assume the hole to exist of concentric ellipses.

The colour of the middle ellips gives the thickness of the SiO_2 layer left. This determines the depth of the hole.
The colour of another ellips determines, beside the local thickness of the SiO_2 layer, its distance normal to the bottom of the hole. So the normal distances of the ellipses to each other are determined by their colour too.

The volume of the etched holes can be approximated by firstly measuring the principal axes of some fixed ellipses*. With these axes the surface area of the ellipses can be calculated.

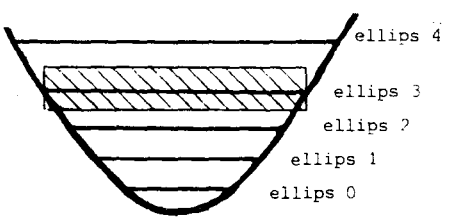

fig. 3.8. : Determination of the etched volume. Explanation see text.

Then, secondly, by determing the distance between the point halfway between e.g. ellips 2 and 3 and the point halfway between ellips 3 and 4 (see figure 3.8.).
If this distance is multiplied by the surface area of ellips 3, a volume is obtained which is shaded in figure 3.8..
If this is done for all fixed ellipses and the obtained volumes are summed, this gives an approximation of the etched volume.

*Fixed ellipses are those chosen to serve as a reference for the determination of the etched volume. Their normal distances are not identical. They were selected for their clear apparent colour.

For the thickness of the elliptical cylinder of ellips 0 (see fig.3.8.) half the distance between ellips 0 and ellips 1 is taken.

For the calculation of the volume of the upper elliptic cylinder a problem arises. The principal axes of the ellips with the colour of the surface, the uppermost ellips, are not obtainable. The transition is too vague. The values of these axes are approximated by extrapolation from the two ellipses lying beneath the top (ellips n-1 and n-2 in figure 3.9.). For the thickness of the top elliptic cylinder half the distance from the surface to the first fixed ellips beneath the surface is used. This leads to the shaded area in figure 3.9..

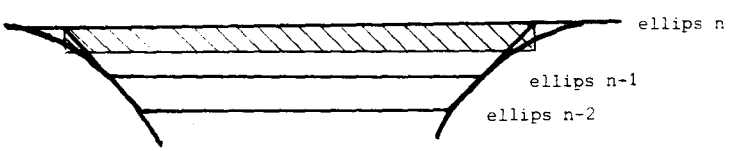

fig. 3.9. : Determination of the volume of the upper elliptic cylinder.

Another problem arises when the etch process has continued into the Si substrate. Then the profile of the walls of the hole in the Si substrate is unknown. No coloured rings are available. This profile is approximated by a parabola of the form

$$y = a.x^2 + b \qquad (3.1)$$

with y : depth.
x : radius from the centre of the paraboloïd to the wall.
a,b : constants.

The constants a and b are determined with the principal axes of the smallest ellips (silver) at height y=0 and the first fixed coloured ellips.

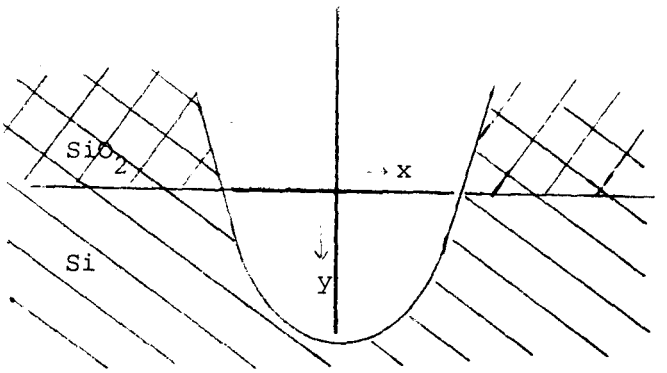

fig. 3.10. : The determination of the etched volume in the Si substrate. Explanation see text.

Because an ellips has two principal axes most of the time two different values for both constants are obtained. In these cases the mean values were used. The extra volume is obtained nearly in the same way as described above for SiO_2. However, the ellipses become circles and the distances between them are chosen 100 Å. The diameter of the circles is obtained with the formula of the determined parabola.

3.2. : The dependence of the etchrate on the accelerating voltage.

In table 3.2. the results of the measurements are given.

Table 3.2. : The results of the measurements. Depth and volume are determined as described in par. 3.1.3.

Target	Accelerating voltage P.E.	Current	Time	Incident charge	Depth	Volume	Type
	(V)	(μA)	(min)	(μA.min)	(Å)	(mm^3)	*
	± 20 V	± 10 μA	±1 min	$x\ 10^3$ $\pm 3.10^3$ (μA.min)	± 150 (Å)	$x\pi.10^{-4}$	
A	2000	726	62	45	1550	4.6±0.3	1
B	2100	795	83	64	6050	32 ± 1	1
C	2200	763	71	54	3900	18 ± 1	1
D	2300	781	90	70	2650	Δ	1
E	2400	786	79	62	2650	6.5±0.3	1
F	2500	266	89	24	750	0.27±0.03	1
G	2500	708	90	64	1550	2.9±0.2	1
I	1700	758	90	68	0	0	2
J	2000	501	107	54	3560	11 ± 1	2
K	1800	744	74	55	0	0	2
L	1900	714	80	57	0	0	2
M	2000	242	86	21	250	0.05 **	2
N #	2300	697	87	61	5200	23 ± 1	2

* Target type 1 : SiO_2 layer of 4650 Å.
2 : SiO_2 layer of 3250 Å.

** Beside the surface colour only one other colour was clearly visible so no proper volume determination (see par. 3.2) could be done.

Δ This preperate was broken so no proper volume determination was possible.

\# During the etching process of this target there was no extra oxygen inlet.

Because a proportionality of the etchrate to the number of incident electrons is expected, the depth respectively the volume are put versus the accelerating voltage for the most similar values of incident charge Q in figure 3.11 and 3.12. Note that in figure 3.12 the volume of D is not displayed. This preparate was broken so only the depth could be measured properly.

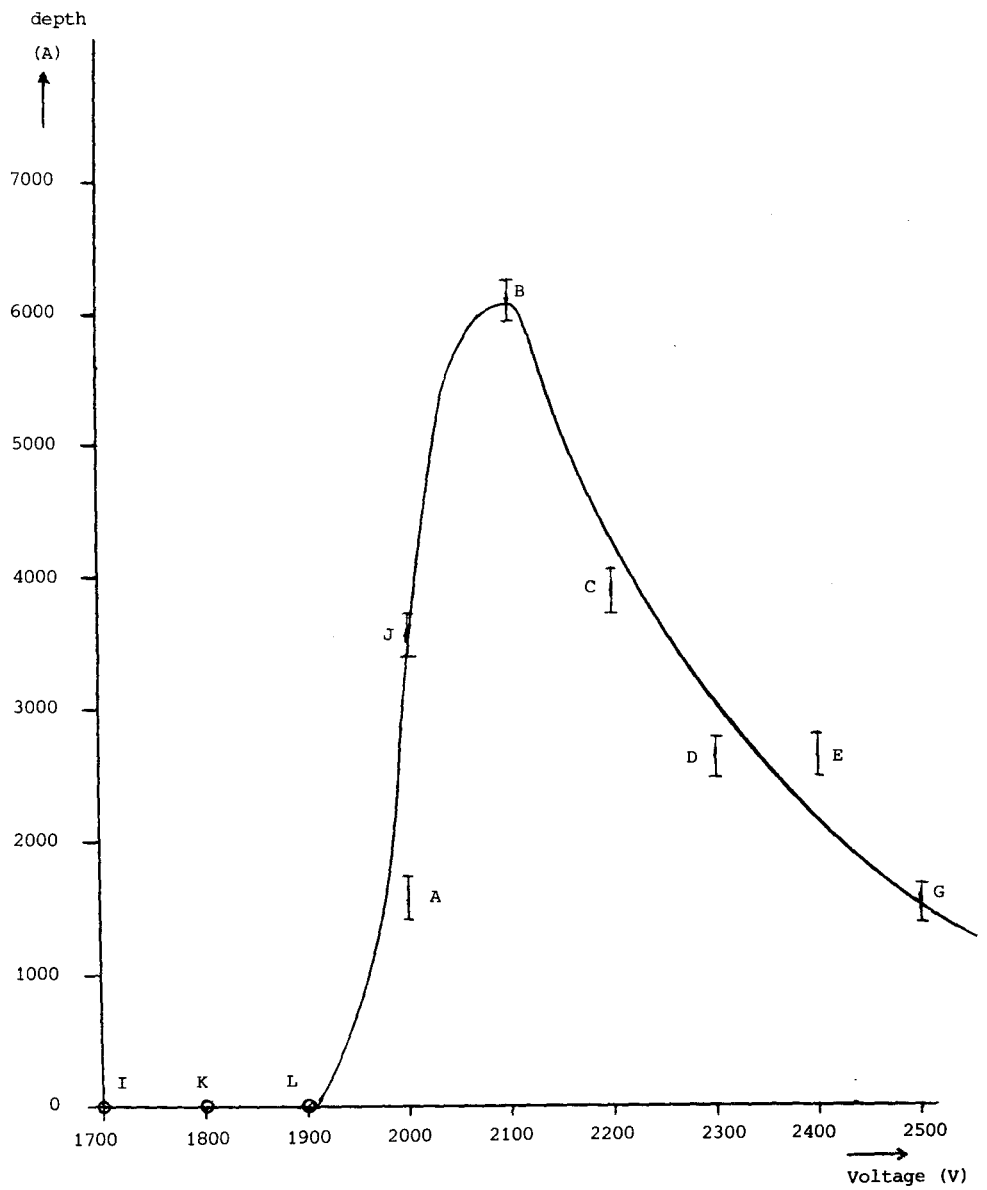

fig. 3.11. : The etched depth versus the accelerating voltage. The curve is drawn through the points with the most similar values of incident charge Q : $54.10^3 \leq Q \leq 70.10^3$ (μA.min).

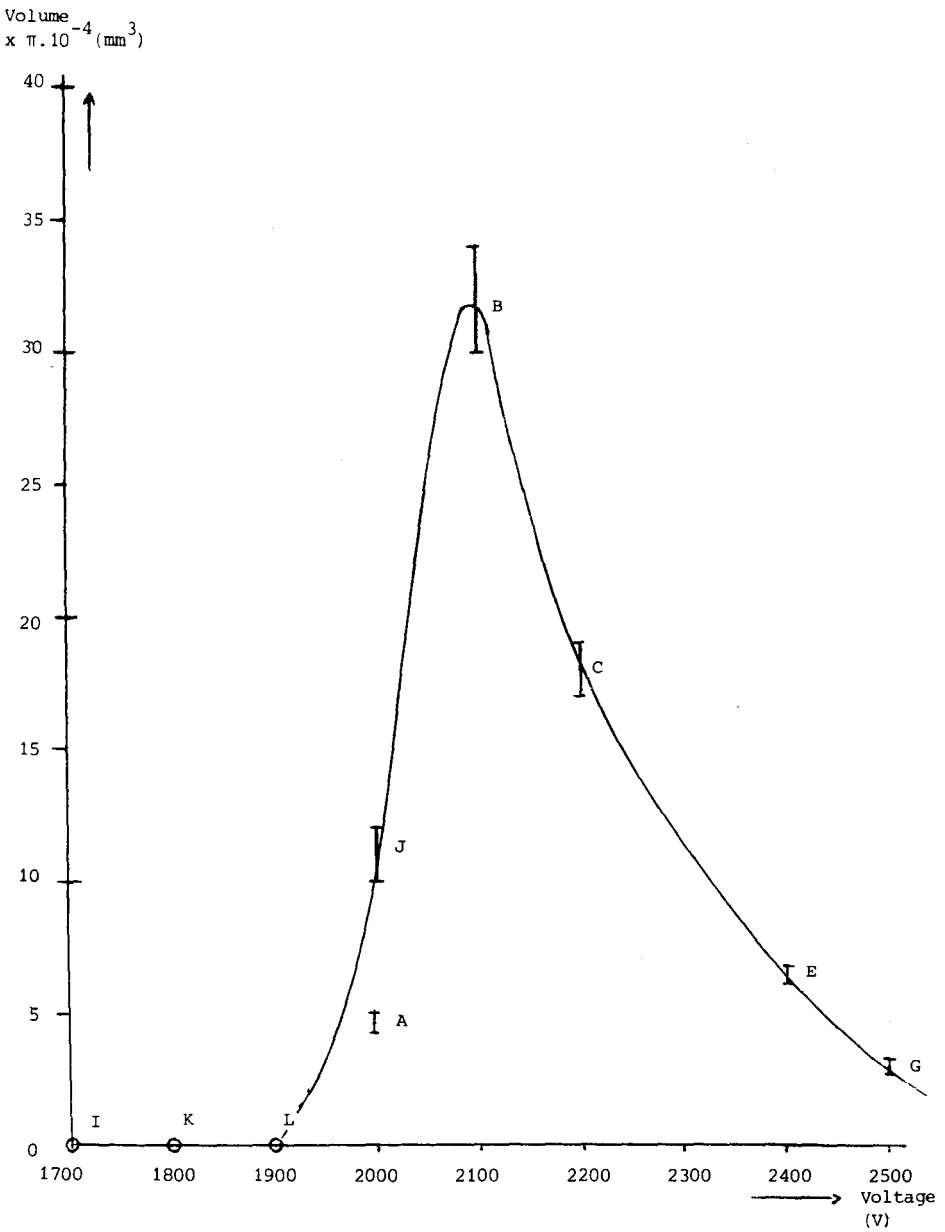

fig. 3.12. : The volume versus the accelerating voltage. The curve is drawn through the points with the most similar values of the incident charge Q : $54.10^3 \leq Q \leq 70.10^3$ (μA.min).

The shape of these curves is remarkable. Below 1900 V no etching occurs. Between 1900 and 2000 V there is a sharp increase in the etched depth respectively the etched volume. This is followed by a less sharp, but still strong decrease from 2100 to 2500 V.

It must be noted that the targets A, B, C, D, E and G are of type 1 and the others, I, J, K and L are of type 2.

The SiO_2 of the surface of targets of type 1 is formed by chemical vapour deposition. The SiO_2 of the surface of the type 2 targets is thermally grown. Because the SiO_2 layers of both types differ in density, type 1 has a lower density then type 2, a better measure for the etchrate would be the number of removed SiO_2 molecules. However, the density of the type 1 target is unknown, so the volume approximation is the best we can do. Because the density of the two types will most likely differ less then 10 % the error will not be too large.

The sharp increase between the 1900 and 2000 V might be explained as follows. From the model (par. 1.3.) it is known that the sign of the surface charge determines whether etching takes place with positive or negative ions. F^- ions would have to etch the surface, if etching occurs, if the surface is charged positively. This occurs if the incident P.E. have an energy between the points E_{pI} and E_{pII} (see fig. 3.13.).

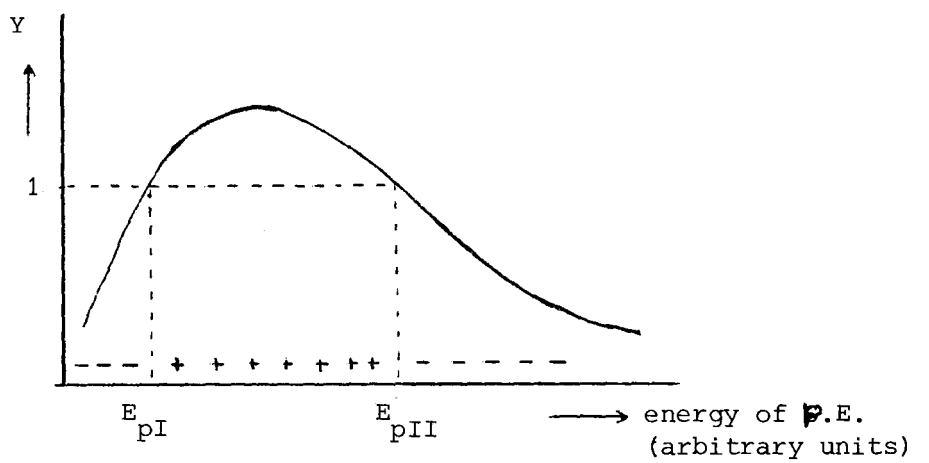

fig. 3.13. : The sign of the charge of the surface for different accelerating voltages (see also fig. 1.10.).

If the surface charges negatively F^+ ions would have to etch the surface. This occurs if the energy of the incident P.E. is initially larger than E_{pII}.

Although the value of E_{pII} is unknown for these surfaces, it lies somewhere between the 1400 and 2300 eV (see chapter 1 figure 1.6. and table 1.1.). The exact value depend, as described in chapter 1, on many things.

From the plasma etching process it is known that F^+ ions are able to etch the SiO_2. Whether F^- ions are able to etch the SiO_2 is unknown. If however, both F^+ and F^- ions etch SiO_2 a sharp increase, such as the one between 1900 and 2000 V in this experiment, could not occur. The sharp increase can be explained if two things are assumed. Firstly, the value of E_{pII} lies somewhere between 1900 and 2000 eV for both preparate types and secondly the F^- ions cannot etch the surface. The reason why only F^+ ions can etch could be that an energy of about 17 eV is set free if an F^+ ion captures an electron. If an F^- ion would have to give away an electron this costs about 4 eV.

The decrease of the curve at higher voltages (above 2100 V) is difficult to explain.

First it must be said that a charging of the surface, with respect to the substrate, of more then 50 V will lead to a breakdown. This breakdown will last only a very short time and is only a local phenomenon. It equalizes the potential difference between the surface and the substrate.
However, the target as a whole, surface plus substrate, is floating with respect to ground so it can easily charge a couple of hundreds of volts with respect to ground. The eventually occuring damage of the surface layer due to some succesive breakdowns is invisible because their direction and place are the same as that of the etching process.

A possible explanation for the decreasing of the etchrate at higher accelerating voltages could be that the waste products of the etching process stick better at the surface if a larger surface charge is present. This better sticking could prevent fresh etchgas molecules from adsorbing at the surface and thus slow down the etchrate.

3.3. : The dependence of the etchrate on the total amount of incident charge.

The model predicts a linear dependence of the etchrate on the number of incident P.E. and thus on the value of the total amount of charge Q incident during the process.

Since the etchrate also depends on the accelerating voltage (see former paragraph) the linearity can only be tested at a fixed accelerating voltage. For 2000 V three values of Q are available. For the other accelerating voltages two or even only one value is known.
Although the number of 3 values is too small to draw founded conclusions an idea of the depence of the etchrate on Q can be given. In figure 3.14. the etched volume versus Q is displayed.

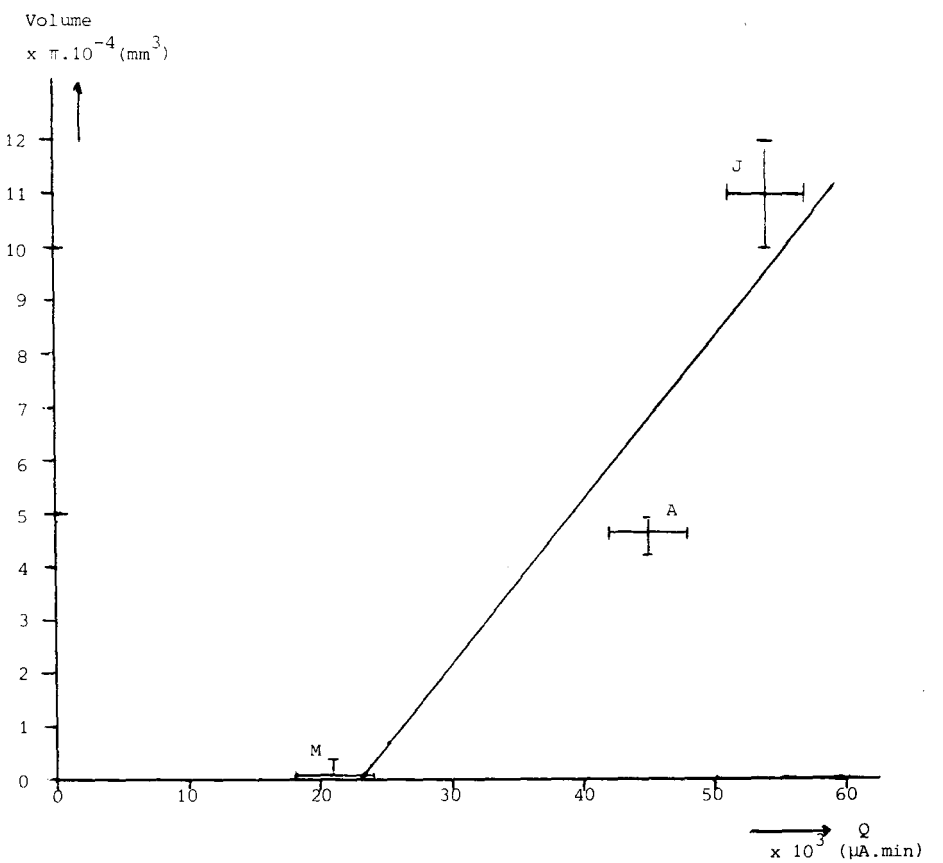

fig. 3.14. : The dependence of the etchrate on the total amount of incident charge Q.
V = 2000 V.

Through three points both a parabola and a regressive line can be drawn. If for the parabola the formula is used :

$$Vol. = a.Q^2 + b.Q + c \qquad (3.2)$$

with : Vol. : the etched volume in units of $\pi.10^{-4}$ mm³.

Q : the total amount of incedent charge during the etching process, in units of 10^3 µA.min.

a, b, c : constants to be determined.

then for a, b and c we obtain the values :

$a = 0.02 \pm 0.09$

$b = -1 \pm 5$

$c = 11 \pm 90$

The values are so inaccurate that no conclusions may be drawn.

For the equation of the straight line one can use the equation :

$$Vol. = m.Q + p \qquad (3.3)$$

with : Vol. : the etched volume in units of $\pi.10^{-4}$ mm³.

Q : the total amount of incident charge during the etchprocess in units of 10^3 µA.min.

m, p : constants to be determined.

For m and p the values

$m = 0.3 \pm 0.1$

$p = -6.9 \pm 3.8$

This linear curve is drawn in figure 3.14.

If this line would hold for the etchprocess this would imply an offset with respect to Q for the etching process. This offset would be in the order of 23.10^3 µA.min. This could imply that a certain amount of charging of the surface is needed before the etching process starts. In that case the offset must be the same for different accelerating voltages. Alas no other measurements are available.

So, although an offset for the etching process with respect to Q is possible, no hard evidence can be given yet. Future research will have to test this statement.

3.4. : The efficiency of the process.

The efficiency of the process can be defined as the quotient of the number of removed SiO_2 molecules and the number of incident P.E. (η = N(removed SiO_2)/N(P.E.)).

With the results of table 3.2. and the knowledge of the number of SiO_2 molecules per mm^3 it is easy to calculate the efficiency. Assume (see par. 3.2.) that both types of targets have the same density namely $2.3\ 10^{19}$ molecules/mm^3. Then the efficiencies as displayed in table 3.3. are obtained.

Table 3.3. : Efficiency of the etching process.

Target	Accelerating voltage (V)	Number of removed SiO_2 molecules $\times 10^{17}$	Number of incedent P.E. $\times 10^{19}$ $\pm$ 0.1 10^{19}	Efficiency η $\times 10^{-3}$
A	2000	0.3 ± 0.02	1.7	1.8 ± 0.2
B	2100	2.3 ± 0.2	2.4	9.6 ± 1.2
C	2200	1.3 ± 0.2	2.0	6.5 ± 0.9
E	2400	0.5 ± 0.02	2.3	2.0 ± 0.2
F	2500	.02 ± .003	0.9	0.2 ± 0.03
G	2500	0.2 ± 0.02	2.4	0.9 ± 0.1
J	2000	0.8 ± 0.08	2.0	4.0 ± 0.6
M	2000	.004	0.8	.05
N *	2300	2.4 ± 0.1	2.3	10.4 ± 1.4

* During the etching process of this target there was no additional inlet of oxygen.

In figure 3.15. the efficiency versus the accelerating voltage is displayed. The curve is drawn through the points with the most similar numbers of incident P.E. As expected, this curve does not differ from the one in figure 3.12. But one point is remarkable, the position of target N. This point lies significantly above the curve although the number of incident P.E. is similar to that of the points on the curve. The difference between the targets on the curve and target N is that during the etching process of all the other targets the background pressure of O_2 was about 2.10^{-5} Torr (see par. 2.2.). This was not the case for target N. It looks as if the extra O_2 has a negative influence on the etching process.

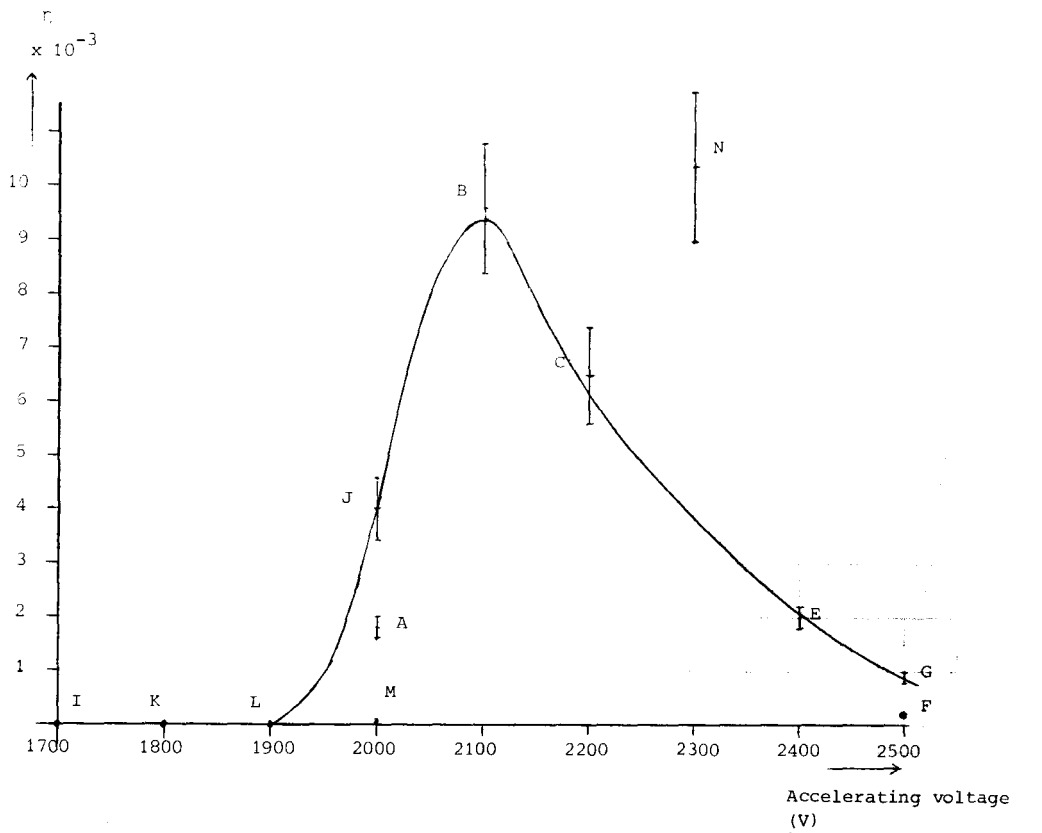

fig. 3.15. : The efficiency versus the accelerating voltage. The curve is drawn through the points with the most similar Q values and O_2 inlet.

Probably the adsorption of O_2 gasmolecules prevents an immediate adsorption of fresh etchgas molecules. Another possible explanation could be that the adsorbed O_2 molecules influence the emission of S.E. in such a way that less F^+ ions are formed.

To obtain a clear view, more research is necessary.

Whether the partial pressure of the etchgas is a limiting factor for the efficiency, can easily be calculated.

Assume a monolayer of SiO_2 is 3 Å thick. Take an etched depth of 6250 Å and the etchtime 83 minutes (target B). This then means that 0.4 monolayers SiO_2 per second are removed in the etching process.

At a pressure of 10^{-4} Torr the monolayer formation time is about 10^{-2} seconds. This means that the maximum number of monolayers formed per second is 100. Now, assume firstly that a monolayer consists for 90 % of T.F.A.A. molecules and secondly that the number of SiO_2 molecules per cm^2 equals the number of molecules in the monolayer per cm^2 and thirdly that 4 T.F.A.A. molecules are needed to remove 1 SiO_2 molecule.
Then the maximum etching velocity would be, if 100 % efficiency was obtained, $\frac{100}{4} \times 0.9 = 23$ monolayers of SiO_2 per second.

Conclusion, the pressure might be lowered a factor $\frac{23}{0.4} = 58$ before it would limit the efficiency. This would mean a pressure of $3.4\ 10^{-6}$ Torr.

Chapter 4 : Conclusions and recommendations.

4.1. : The applicability of the electron-beam etching process.

There are two factors that influence the applicability of the process. These are the maximum reachable accuracy and the velocity of the etching process.

4.1.1. : The accuracy of the etching process.

The accuracy of the etching process depends on the strength and the direction of the forces working on the produced ion. They determine the distance the ion can travel before it impacts on the surface. These forces are Coulomb forces. They originate from the charge of the ion and from the charge in and on the surface.

Consider the following rough model (see fig. 4.1.).

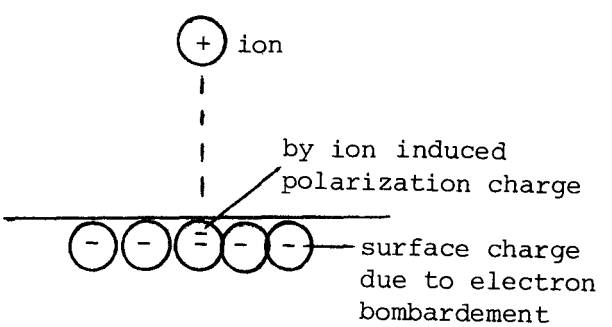

fig. 4.1. : A drawing of the situation used in the model for the calculations of the forces working on the produced ion.

We only consider the interactions of the ion with an atom straight below it, in the surface.

Let us first consider the interaction of the ion with the induced polarisation charge.

The electric field strength in free space due to a charge q is :

$$E = \frac{q}{4\pi\varepsilon_o r^2} \qquad (V.m^{-1}) \qquad (4.1)$$

with q : elementary charge.(C)

ε_o : permittivity of vacuum.($C^2.N^{-1}.m^{-2}$)

r : distance from the charge.(m)

Because we only consider the interaction of the ion with the atom straight below, this surface atom can be thought of as exposed to a homogeneous electric field. This induces a polarisation of the atom with polarisation charge :

$$Q_{surf} = \frac{\sigma_p}{N_{surf}} = \frac{-\varepsilon_o(\varepsilon_r - 1).E}{N_{surf}} \qquad (C.atom^{-1}) \qquad (4.2)$$

with σ_p : polarisation charge density.($C.m^{-2}$)

ε_r : relative permittivity of the surface material.

N_{surf} : number of surface atoms per m^2.

Q_{surf} : polarisation charge on 1 surface atom.($C.atom^{-1}$)

So the ion feels an attractive force due to the interaction of its own charge with the induced polarisation charge of :

$$F_{pol} = \frac{Q_{surf}.q}{4\pi\varepsilon_o} \cdot \frac{1}{r^2} \qquad (N) \qquad (4.3)$$

with F_{pol} : the attractive force on the ion due to the polarisation charge on the surface.

With the aid of (4.2) and (4.1) this leads to :

$$F_{pol} = \frac{(\varepsilon_r - 1).q^2}{16\pi^2.\varepsilon_o.N_{surf}} \cdot \frac{1}{r^4} \qquad (N) \qquad (4.4)$$

$$= \frac{K}{r^4}$$

with K : $\dfrac{(\varepsilon_r - 1).q^2}{16\pi^2.\varepsilon_o.N_{surf}}$ $\qquad (N.m^4)$

This force is proportional to r^{-4}. So, though it may be large at small distances above the surface, it rapidly decreases with increasing distance.

Let us now consider the force due to the charge in and on the surface, which is originated by the incident P.E. Assume, as an approximation, that the charge is concentrated in the toplayer of the surface. The amount of charge on the surface is then equal to :

$$Q = V.C \qquad (C) \qquad (4.5)$$

with Q : the amount of charge on the surface.(C)
V : the potential of the surface with respect to ground.(V)
C : the capacity of the surface.($C.V^{-1}$)

Because here again we look only at the interaction of the ion with the surface molecule right underneath it, we must calculate the charge per surface molecule. This is :

$$Q_{surf.ch} = \frac{V.C}{N_{surf}} \qquad (C) \qquad (4.6)$$

with $Q_{surf.ch}$: the charge on a surface molecule due to the charging of the surface by the electron-beam.

The force due to this charge is :

$$F_{ch} = \frac{Q_{surf.ch}.q}{4\pi.\varepsilon_o.r^2} \qquad (N) \qquad (4.7)$$

$$= \frac{V.C.q}{4\pi.\varepsilon_o.N_{surf}} \cdot \frac{1}{r^2} \qquad (N) \qquad (4.8)$$

$$= \frac{M}{r^2} \qquad (N)$$

with M : $\frac{V.C.q}{4\pi.\varepsilon_o.N_{surf}}$ $\qquad (N.m^2)$

The total force felt by the ion, in this simple model, is :

$$F_{tot} = F_p + F_{ch} \qquad (N) \qquad (4.9)$$

$$= \frac{K}{r^4} + \frac{M}{r^2} \qquad (N) \qquad (4.10)$$

Assume the following situation :
An F^+ ion is originated at 4 $\mathring{A}$ above the surface (the length of the T.F.A.A. molecule). It is propelled away with an energy of 1 eV at an angle of 45 degrees with the surface. The energy is a These data are certainly not worst case, but seem to be a realistic starting point for a first approximation.
In addition to this we assume that the capacity of the surface is 1 pF (a low value but in the right order) and the potential is -100 V.

The interesting thing to know is how long it will take before the ion impacts at the surface. This determines the horizontally travelled distance and thus the accuracy of the etching process. To obtain this time of flight we only have to look at the vertical motion of the ion. The equation to be solved for this is :

$$m.\frac{d^2r}{dt^2} = -\frac{K}{r^4} - \frac{M}{r^2} \qquad (4.11)$$

with m : the mass of the ion.(kg)
r : the distance to the surface
K, M : as indicated in respectively (4.4) and (4.8)
and initial values of

$$r(0) = 4.10^{-10} \text{ m}$$
$$v(0) = 2.25\ 10^{3} \text{ m.s}^{-1}$$

This differential equation is solved numerically with a Runga Kutta method (VEL79). The extra differential equation used was

$$\frac{dx}{dt} = v \qquad (4.12)$$

The values of K and M were respectively $2.37\ 10^{-22}$ (Nm^4) and $4.5\ 10^{6}$ (Nm^2).

The calculated time of flight is of the order of 10^{-18} sec. So the by the ion horizontally travelled distance is in the order of 10^{-15}m.
Note that this time and distance are so small that one must question the applicability of this model. Quantum mechanical effects will play an important role then.
However, one might safely conclude that probably the beam diameter of the electron beam will be the limiting factor in the obtainable accuracy in the etching process.

4.1.2. : The speed of the etching process.

The speed of the etching process is a second interesting property from the point of view of applicability. At the moment it is possible to make electron beams with a diameter of about 0.1 μm and a beamcurrent of 0.1 μA at an accelerating voltage of 2000 V. This means a power density of 2.5 10^{10} W.m^{-2}. To see whether such beams can be used in the etching process we have to investigate whether the SiO_2 layer will melt or not if that amount of power is used.
This can be calculated with the model indicated in figure 4.2.

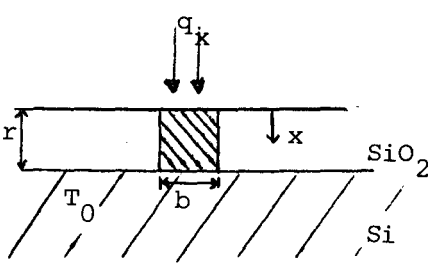

q_x = power density.

T_0 = temperature of the Si substrate.

fig. 4.2. : The starting points of the model used to calculate the local heating of SiO_2.

Because the thickness of the SiO_2 layer is much smaller than that of the Si substrate, in first approximation, the temperature of the substrate is thought to be constant T_0.

Further, because b is of the same order as r (see fig. 4.2.), we neglect radial thermal conduction. As a last approximation we neglect loss of heat by thermal radiation. These assumptions lead to an overestimation of the temperature raise.
Due to these assumptions the problem becomes the one dimensional one displayed on figure 4.2. For the stationary situation we obtain (SCH00) the equation :

$$q_x = -\lambda.\frac{dT}{dx} \qquad (W.m^{-2}) \qquad (4.13)$$

with q_x : power density.$(W.m^{-2})$
λ : thermal conductivity of the material.$(W.m^{-1}.K^{-1})$
$\frac{dT}{dx}$: the temperature gradient in the x-direction (see fig.4.2.). $(K.m^{-1})$

This leads in our situation to :

$$T_{surf} - T_0 = \frac{q_x.r}{-\lambda} \qquad (K) \qquad (4.14)$$

with T_{surf} : surface temperature in the stationary situation.(K)

For $q_x = -2.5\ 10^{10}\ W.m^{-2}$
$r = 10^{-7}\ m$
$\lambda = 8.8\ W.m^{-2}.K^{-1}$

this leads to $T_{surf} - T_0 = 284\ K$.

Although this will not melt the SiO_2 layer it might be too high if the adsorption of the etchgas is considered. To see whether this staionary situation is reached we have to calculate the time necessary to etch the hole down to the Si substrate. With this time we can calculate the amount of heat put into this cylinder and see whether this is sufficient to establish the stationary situation. The time necessary to etch the hole is :

$$t = \frac{(\pi/4).b^2.r.n.q}{\eta.i} \qquad (sec) \qquad (4.15)$$

with b,r : as indicated in fig. 4.2.(m)
n : number of molecules per m^3. (m^{-3})
q : the elementary charge.(C)
η : efficiency of the etching procss.
i : beam current.(A)

For $b = 10^{-7}$ m $q = 1.6\ 10^{-19}$ C
$r = 10^{-7}$ m $\eta = 10^{-2}$
$n = 2.3\ 10^{28}$ m^{-3} $i = 10^{-7}$ A

the etching time is $2.9\ 10^{-3}$ seconds. During this time an amount of $2000.10^{-7}.\ 2.9\ 10^{-3}$ (V.A.s) = $5.8\ 10^{-7}$ J is brought into the cylinder.

To obtain the stationary temperature the necessary amount of heat is :

$$Q = C.m.\Delta T \qquad (J) \qquad (4.16)$$

with C : heat capacity of the surface material.($J.kg^{-1}$)
m : the mass of the cylinder.(kg)
ΔT : the temperature increase.(K)

For SiO_2 : $C = 0.98\ \ 10^{3}\ J.kg^{-1}$.
$m = 1.81\ 10^{-18}$ kg. (Specific density of $2.3\ 10^{3}$ $kg.m^{-3}$ and a volume of $7.85\ 10^{-22}$ m^{3})
$\Delta T = 142$ K. (The mean value of ΔT over the thickness of the surface layer)

the necessary amount of heat is $2.5\ 10^{-13}$ J. This means that the stationary situation is reached very quickly.

With the knowledge from above we can make an approximation of the time necessary to etch a certain volume.
For instance what time would it cost to etch a surface area of half a wafer with a diameter of 2 inch and a surface layer thickness of 1000 $\mathring{A}$? Say that we use a beam burrent of 10^{-8} A and a diameter of 10^{-7}m. The etching time then is :

$$t = \frac{Volume.q.n}{\eta.\ i} \qquad (sec) \qquad (4.17)$$

For : Volume = $5.08\ 10^{-11}$ m^{3} $i = 10^{-8}$ A
$q = 1.6\ 10^{-19}$ C $\eta = 10^{-2}$
$n = 2.3\ 10^{28}$ m^{-3}

the etching time is about 500,000 hours. This of course is too much for practical applications.

Concluding to this paragraph it can be said that although high resolutions are obtainable with the electron-beam etching technique the etching time for large surface areas is too large. This long etching time is inherent to the local character of the etching process. A reduction of the time could be obtained if more electron beams are used at the same time and/or the surface layer of SiO_2 is made thinner.

Further research has to find out the possibilties to reduce the etching time.

4.2. : Recommendations for further research.

If follow up research takes place, the experimental arrangements must at least meet the following specifications :

- an electron gun with good focussing properties, a stable beam current and a tunable spot must be used.
- an instrument with which the size of the elctron beam, incident on the target, can be measured must be present. Such an instrument can easily be made of two conducting wires just above or beside the target.
- vacuumpumps must be used which do not produce vapours of their own. So for instance no oil diffusion pump must be used.
- a mass spectrometer must be present to keep track of the composition of the gas in the vacuum system.
- an etchgas supply system, like glass, which does not react with the etchgas must be build. This avoids the dillution of the container with the etchgas.
- a method must be found by which the gasflow of the etchgas into the system is kept constant (see par. 3.1).
- a heater for cleaning the target in an O_2 atmosphere in the same vacuum as where the etching process will take place.

Two other recommendations for the experimental arrangements are not as necessary as the ones mentioned above. The first is that it would be nice if the vacuum system existed of two chambers seperated by a wall with a small hole. One chamber for the electron gun and one for the target where the etching process takes place. The etchgas is only necessary in the target chamber. If these chambers are differentially pumped the electron gun could be operated at stable pressure conditions. The pressure variations in the target chamber do not influence the beam current nor does the etchgas react with e.g. the filament of the electron gun. The second arrangement would be an instumrument with which the etching process can be followed dynamically. This would considerably cut experimental time.

From the point of view of the applicability interesting research subjects are :

- The dependence of the etchrate on the inlet of oxygen. From figure 3.15 in paragraph 3.4 it looks as if the oxygen influences the etchrate negatively. So it is important to investigate the shape of the curve if there is no O_2 inlet during the etching process. Maybe it is possible to find a gas that increases the etchrate.
- The dependence of the etchrate on the total amount of incident charge must be looked at more accurately and must be tested for different accelerating voltages. This could give clarity for the question if there really exists an offset.
- The dependence of the etchrate on the structure of the SiO_2 layer must be investigated too. Impurities in the surface layer can influence the production of S.E. in a negative way.
- The dependence of the etchrate on different etchgasses. T.F.A.A. is extremely agressive. Probably there are less agressive and/or more effective etchgasses that can be used.
- The thickness of the SiO_2 layer can probably be reduced. The etching process is a local one so the SiO_2 layer does not have to protect the substrate against impact of energetic ions like in the plasma etching technique. It only serves as a mask for e.g. diffusion. So the SiO_2 layer must be thick enough to prevent the diffusion process from reaching the Si substrate through the SiO_2 layer.
- The way of how one can etch the SiO_2 layer up to the Si substrate without etching the Si must be investigated too. Maybe it it possible to work out a mechanism that controls the motion of the electron beam in such a way that damage of the Si substrate is prevented.
- Because of the long etching time it is worthwhile to investigate the possibility of using more electron beams at the same time.
- Fundamental research must show how the etchgas molecule sticks at the surface and which reaction products are formed. The efficient removal of these products from the surface must be studied too.

Literature :

BAU 69 : Tabellen boekje voor onderwijs in de natuur- en scheikunde. 2nd edition.
Editors : H.Ph.Baudet, J.Ph.Steller and R.E.F.Zweers.
Wolters-Noordhoff 1969.

BOW 82 : H.Bowker, H.Houghton and K.C.Waugh.
The Interaction of Acetaldehyde and Acetic acid with the ZnO surface.
Journal of Catalyses, 79, 431-444 (1983).

BRO 83 : Eigenschappen van de vaste stof.
Authors : Prof.dr. H.H.Brongersma and Dr. R.M.A.Lieth.
Syllabus of the Technical University of Eindhoven.
Syllabusnumber : 3.415 (1983).

BRU 38-1 : H.Bruining.
Secondary Electron Emission part II : Absorption of Secondary Electrons.
Physica, 5, 901 (1938).

BRU 38-2 : H.Bruining.
Secondary Electron Emission part III : Sekondary Electron Emission caused by slow Primary Electrons.
Physica, 5, 913 (1938).

COB 79 : J.W.Coburn and H.F.Winters.
Plasma Etching - A Discussion of Mechanisms.
Journal of Vacuum Science, 16, 391-403 (1979).

DEK 54 : A.J.Dekker.
Energy and Temperature Dependence of the Secondary Emmision of MgO.
Physical Review, 94, 1179 (1954).

FLA 81 : D.L.Flamm, V.M.Donnelly and J.A.Mucha.
The Reaction of Fluorine Atoms with Silicon.
Journal of Applied Physics, 52, (5) (1981).

GIB 51 : J.H.Gibbs and C.P.Smyth.
Dipole Moment, Induction and Structure in Four Fluorine-substituted Molecules.
Journal of the American Chemical Society, 73, 5115-5116 (1951).

GIB 66 : Handbook of Vacuum Physics, part 3 : Secondary Electron Emission.
D.J.Gibbons.
Editor : A.H.Beck
Pergamon Press, Oxford (1966).

JON 51 : P.H.L.Jonker.
The Angular Distribution of the Secondary Electrons of Nickel.
Philips Research Reports, 6, 202, (1937).

JOH 53 : J.B.Johnson and K.G.McKay.
Secondary Electron Emission of Crystalline MgO.
Physical Review, 91, 581 (1953).

KAL 78 : H.Kalter and E.P.G.T. van de Ven.
Plasma Etching in I.C.-technology.
Philips Technical Review, 38, 200-210 (1979).

KAR 44 : J.Karle and L.O.Brockway.
An Electron Diffraction Investigation of the Monomers and Dimers of Formic-, Acetic- and Trifluoroacetic Acid and the Dimer of Deuterium Acetate.
Journal of the American Chemical Society, 66, 574-584 (1944).

KEL 78 : J.J.Kelly and G.J.Koel.
Galvanic Effects in the Wet-chemical Etching of Metal Films.
Philips Technical Review, 38, 147-157 (1978/79).

KNO 39 : M.Knoll and R.Theile.
Elektronenabtaster zur Struktur Abbildung von Oberflächen und dünnen Schichten.
Zeitschrift für Physik, 113, 260 (1939).

KOL 37 : R.Kollath.
Sekundärelektronen Emission fester Körper.
Physikalisches Zeitschrift, 38, 202 (1937).

KOL 56 : Handbuch der Physik.
Sekundärelektronen Emission fester Körper bei Bestralung mit Elektronen.
R.Kollath (1965).
Universitäts drückerei H.Stürtz A.G.,Würtzberg.

MAL 56 : Malcolm B.Templeman and Moddie O.Taylor.
The Vapor Phase Dissociation of Some Carboxylic Acids III : Trifluoroacetic acid and Trifluoroacetic Acid-d.
Journal of the American Chemical Society, 78, 2950-2953 (1956).

PET 60 : B.Petzel.
Measurements of the Secondary Emission of KCl and KBr.
Radio Enginering and Electronics, 5, 133 (1960).

POL 80 : J.v.d.Pol.
Handleiding van de elektronenstraal-verdampings vacuüminstallatie, en het verdampingsproces voor het maken van dunne poly-silicium lagen.
T.H. Eindhoven (1980).

REI 77 : Raster Electronen Microscopie.
L.Reimer and G.Pfefferhorn.
Springer Verlag, Berlin (1977).

SCH 00 : Fysische Transportverschijnselen.
Dr.ir. P.P.J.M.Schram and Ir. P.T.Smulders.
Syllabus of the Technical University of Eindhoven.
Syllabusnumber : 3.322.

VEL 79 : Numerieke Methoden I en II.
Prof.dr. G.W.Veltkamp and Drs. A.J.Geurts.
Syllabus of the Technical University of Eindhoven.
Syllabusnumber : 2.211 (1979/80).

WOO 40 : D.E. Woodridge
Temperature Effects in Secundary Emission
Physical Review, 58, 316-321 (1940)

WEA 81 : Handbook of Chemistry and Physics

Appendix I :

Some properties of CF_3COOH.

- Molecular weight : 114.02 (gr/mol)
- Density : 1.5351 (gr/cm^3)

From : (WEA81)

- Molar volume : 74.275 (cm^3/mol)
- ΔH_{subl} : 38.024 (kJ/mol)
- ΔH_{vap} : 33.259 (kJ/mol)

From : (MAL56)

- Dipole moment : $7.60\ 10^{-30}$ (C.m)

From : (GIB51)

- Dimensions of the molecule

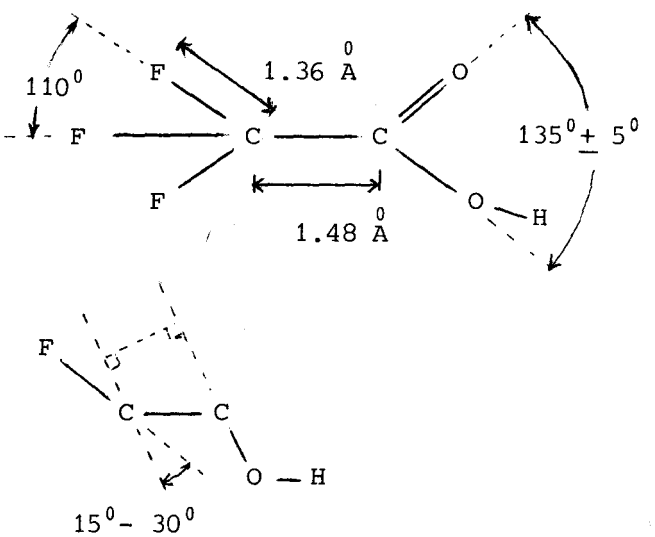

The CF_3 - group rotates freely round the C - C axis.

From : (KAR44)

- The lenght of the molecule can only be calculated if some additional properties are known.
  These are taken from the data of acetic acid obtained by (KAR44).

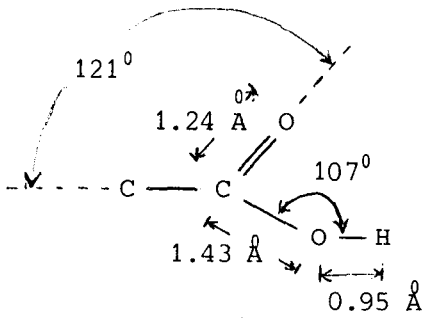

The data for the length of the O - H bond and the C - O - H bond angle are from (WEA81) for formic acid.

Now stereometric calculations for the projection of the C - F bond on the C - C axis give :

$P(C - F) = 0.423 \times \text{length } (C - F)$

$= 0.44 \text{ Å}$

The projection of the C = O bond on the C - C axis has a length of :

$P(C = O) = \cos(180^0 - 121^0) \times \text{length } (C = O)$

$= 0.60 \times 1.24 = 0.74 \text{ Å}$

The C - C - O bond angle = $360^0 - 135^0 - 121^0 = 104^0$.

The projection of the C - O - H group on the C - C axis has a length of :

$P(C - O - H) = \cos(180^0 - 104^0) \times \text{length } (C - C) +$

$\cos(107^0 - 104^0) \times \text{length } (O - H)$

$= 0.37 \times 1.43 + 0.99 \times 0.95 \text{ Å}$

$= 1.47 \text{ Å}$

A total value of 3.39 Å is obtained. The atomic radius of the H - atom must be added twice (at both ends of the molecules).
This radius is 0.29 Å (from : BAU69).
The length of the molecule then is : 3.97 Å

Some properties of SiO_2 :

- Surface energy (fresh) : 4000 (mJ/m^2)
  (old) : 400 (mJ/m^2)
  From : (BRO83)

- Molecular weight : 60.08 (gr/mol)
  Density : 2.3 (gr/cm^3)
  From : (WEA81)

- Molar volume : 26.122 (cm^3/mol)

- The number of surface molecules can be estimated with (BRO83) :

$$N_{surf} = (\rho.N_0/M)^{2/3} \quad (m^{-2})$$

with ρ : density (kg/m^3)
N_0 : Avogadro's number
M : Molecular weight (kg/mol)

This gives :

$$N_{surf}(SiO_2) = 8.1\ 10^{18} \quad (m^{-2})$$

- The distance of the surface molecules is approximately

$$d = (1/N_{surf})^{-1/2} = 3.5\ 10^{-10} \quad (m)$$

Appendix II : Colour chart for thermally grown SiO_2 films.

Observed perpendicularly under daylight fluorescent lighting.

Thickness (microns)	Order (5450 Å)	Colour and Comments
0.05^5		Tan (geelbruin)
0.07^5		Brown
0.10^o		Dark violet to red-violet
0.12^5		Royal blue (diepblauw)
0.15^o		Light blue to metallic blue
0.17^5	I (zwarte band)	Metallic to very light yellow green
0.20		Light gold or yellow-slightly metallic
0.22^5		gold with slight yellow-orange
0.25^o		orange to melon
0.27^5		red violet
0.30^o		blue to violet-blue
0.31^o		blue
0.32^5		blue to blue-green
0.34^5		light green
0.35^o	II (zwarte band)	green to yellow-green
0.36^5		yellow green
0.37^5		green-yellow
0.39		yellow
0.41^2		light orange
0.42^5		carnation pink (vleeskleurig)
0.44^2		violet red
0.46^5		red-violet
0.47^5		violet
0.48^o		blue violet
0.49^o		blue
0.50^2		blue-green
0.52^o		green (broad)
0.54^o		yellow-green
0.56	III	green-yellow
0.57^4		yellow to yellowish (Not yellow but is in the position where yellow is to be expected. At times it appears to be light creamy grey or metallic

- Continued -

Thickness (microns)	Order (5450 Å)	Coulor and Comments
0.58^5		light-orange or yellow to pink borderline
0.60^o		carnation pink
0.63^o		violet-red
0.68		"bluish" (Not blue but borderline between violet and blue-green. It appears more like a mixture between violet-red and blue-green and overall looks greyish)
0.72	IV	blue-green to green (quite broad)
0.77		"yellowish"
0.80	(IV)	orange (rather broad for orange)
0.82		salmon
0.85		dull (=dof), light red-violet
0.86		violet
0.87		blue-violet
0.89		blue
0.92	V	blue-green
0.95		dull yellow-green
0.97		yellow to "yellowish"
0.99		orange
1.00		carnation pink
1.02		violet-red
1.05		red-violet
1.06		violet
1.07		blue-violet
1.10		green
1.11		yellow-green
1.12	VI	green
1.18		violet
1.19		red-violet
1.21		violet-red
1.24		carnation pink to salmon
1.25		orange
1.28		"yellowish"
1.32	VII	sky blue to green blue
1.40		orange
1.45		violet
1.46		blue violet
1.50	VIII	blue
1.54		dull